



**KAUNAS UNIVERSITY OF TECHNOLOGY
FACULTY OF CHEMICAL TECHNOLOGY**

Robertas Tiažkis

**INFLUENCE OF FLUORO AND METHYL GROUPS IN
ORGANIC PHOTOCONDUCTORS CONTAINING
FLUORENYL AND CARBAZOLYL CHROMOPHORES**

Master's thesis

Supervisor

Senior researcher dr. Marytė Daškevičienė

Kaunas, 2017



**KAUNO TECHNOLOGIJOS UNIVERSITETAS
CHEMINĖS TECHNOLOGIJOS FAKULTETAS**

Robertas Tiažkis

**FLUOR- IR METILGRUPIŲ ĮTAKOS FLUORENILO IR
KABAZOLILO CHROMOFORUS TURINČIŲ ORGANINIŲ
FOTOPUSLAIDININKIŲ SAVYBĖMS TYRIMAS**

Baigiamasis magistro darbas

Vadovė

Vyr. m. d. dr. Marytė Daškevičienė

Kaunas, 2017

**KAUNO TECHNOLOGIJOS UNIVERSITETAS
CHEMINĖS TECHNOLOGIJOS FAKULTETAS
ORGANINĖS CHEMIJOS KATEDRA**

TVIRTINU

Organinės chemijos
katedros vedėjas
Prof. dr. Vytas Martynaitis

**FLUOR- IR METILGRUPIŲ ĮTAKOS FLUORENILO IR
KABAZOLILO CHROMOFORUS TURINČIŲ ORGANINIŲ
FOTOPUSLAIDININKIŲ SAVYBĖMS TYRIMAS**

Baigiamasis magistro darbas

Studijų programa Taikomoji chemija (kodas 612F10003)

Vadovė

Vyr. m. d. Marytė Daškevičienė

Recenzentas

Prof. dr. Saulius Grigalevičius

Darbą atliko

Robertas Tiažkis

Kaunas, 2017



KAUNO TECHNOLOGIJOS UNIVERSITETAS
CHEMINĖS TECHNOLOGIJOS FAKULTETAS

Robertas Tiažkis

Studijų programa Taikomoji chemija (kodas 621F10003)

Baigiamojo darbo „Fluor- ir metilgrupių įtakos fluorenilo ir karbazolilo chromoforus turinčių organinių fotopulsaidininkų savybėms“

AKADEMINIO SAŽININGUMO DEKLARACIJA

2017 m. gegužės mėn. 30 d.

Kaunas

Patvirtinu, kad mano **Robertas Tiažkis** baigiamasis darbas tema „*Fluor- ir metilgrupių įtakos fluorenilo ir karbazolilo chromoforus turinčių organinių fotopulsaidininkų savybėms*“ yra parašytas visiškai savarankiškai, o visi pateikti duomenys ar tyrimų rezultatai yra teisingi ir gauti sąžiningai. Šiame darbe nei viena darbo dalis nėra plagijuota nuo jokių spausdintinių ar internetinių šaltinių, visos kitų šaltinių tiesioginės ir netiesioginės citatos nurodytos literatūros nuorodose. Įstatymu nenumatytų piniginių sumų už šį darbą niekam nesu mokėjęs.

Aš suprantu, kad išaiškėjus nesąžiningumo faktui, man bus taikomos nuobaudos, remiantis Kauno technologijos universitete galiojančia tvarka.

(vardą ir pavardę įrašyti ranka)

(parašas)

CONTENTS

SUMMARY	6
SANTRAUKA	7
LIST OF ABBREVIATIONS AND PHYSICAL UNITS	8
1. INTRODUCTION.....	10
2. Literature review	11
2.1. Perovskite solar cells	11
2.2. Properties HTMs containing methyl groups	12
2.3. Properties of HTMs containing fluorine groups	18
2.4. Literature review conclusions	20
3. MATERIALS AND METHODS	21
3.1. Synthesis of the intermediate compounds.....	21
3.2. Synthesis of HTMs	25
4. Results and discussions	37
4.1. HTMs based on fluorene with different aliphatic substitutions.....	37
4.1.1. Synthesis.....	37
4.1.2. Properties.....	40
4.1.3. Conclusions	45
4.2. Fluorinated HTMs.....	45
4.2.1. Synthesis.....	46
4.2.2. Properties.....	49
4.2.3. Conclusions	55
Conclusions.....	56
References.....	57
List of publications.....	61

Tiažkis, Robertas. *Influence of Fluoro and Methyl Groups in Organic Photoconductors Containing Fluorenyl and Carbazolyl Chromophores: Master's thesis in Chemistry* / supervisor senior researcher dr. Marytė Daškevičienė. The Faculty of Chemical Technology, Kaunas University of Technology.

Research area and field: Physical Sciences, Chemistry.

Kaunas, 2017. XX p.

SUMMARY

The molecular structure of hole transporting materials (HTMs) play an important role in hole extraction in perovskite solar cells. It has significant influence on molecular planarity, energy level, and charge transport properties. Understanding the relationship between the chemical structure of HTMs and perovskite solar cells (PSCs) performance is crucial for the continued development of efficient organic charge transporting materials. Using a molecular engineering approach we have constructed a series of hole transporting materials with strategically placed aliphatic substituents to investigate the relationship between the chemical structure of the HTMs and the photovoltaic performance. PSCs employing the investigated HTMs demonstrate power conversion efficiency values in the range of 9% to 16.8% highlighting the importance of optimal molecular structure. An inappropriately placed side group could compromise the performance of the device. Due to ease of synthesis and moieties employed in its construction, it offers a wide range of possible structural modifications. This class of molecules has great potential for structural optimization in order to realize simple and efficient small molecule based HTMs for perovskite solar cell application.

One of the main problems of PSCs is hygroscopicity of the perovskites which determines the transiency of the cells. The second part of this project was to synthesize HTMs which would be more moisture resistant. Because of the unique characteristics of the fluorine atom we decided to construct materials which would have a similar structure to the conventional ones and replacing one or several hydrogen atoms with fluorine atoms. After measuring the wetting angle of the materials we found out that the addition of a fluorine atom in a molecule increased the hydrofobicity of the material almost in all cases. Based on these results we can assume that a strategic addition of fluorine atoms to a HTM could increase the operation time of a PSC.

Tiažkis, Robertas. Fluor- ir metilgrupių įtakos fluorenilo ir kabazolilo chromoforus turinčių organinių fotopulsaidininkų savybėms tyrimas. *Chemijos magistro* baigiamasis darbas / vadovas vyr. m. d. dr. Marytė Daškevičienė; Kauno technologijos universitetas, Cheminės technologijos fakultetas. Mokslo kryptis ir sritis: fiziniai mokslai, chemija
Kaunas, 2017. XX p.

SANTRAUKA

Skylių perovskitiniuose saulės elementuose gavimui svarbų vaidmenį vaidina skyles pernešančių medžiagų (HTM) struktūra, nuo kurios stipriai priklauso molekulės plokštumas, energetiniai lygmenys ir krūvio pernašos savybės. Ryšio tarp cheminės HTM struktūros ir perovskitinių saulės elementų (PSC) veikimo charakteristikų supratimas yra būtinas tolesniam efektyvių organinių krūvį pernešančių medžiagų kūrimui. Šiame darbe HTM struktūros įtakos PSC fotovoltinėms savybėms ištyrimui pasitelkiant molekulinės inžinerijos metodą buvo susintetinta serija naujų organinių medžiagų su alifatiniais pakaitais skirtingose padėtyse. Naudojant šias skyles pernešančias medžiagas sukonstruotų PSC elektros konversijos efektyvumas yra nuo 9% iki 16,8%. Tai patvirtina optimalios molekulinės struktūros svarbą - netinkamoje vietoje prijungta šoninė grupė gali ženkliai pabloginti prietaiso eksploatacines savybes. Dėl sintezės paprastumo ir joje panaudotų pradinių junginių galimas platus organinių fotopulsaidininkų struktūrinių modifikacijų pasirinkimas. Šios klasės junginių struktūros optimizavimas atveria plačias galimybes paprastų ir efektyvių mažų molekulių pagrindu susintetintų HTM panaudojimui perovskitinėse saulės celėse.

Viena iš pagrindinių PSC problemų yra saulės elementų trumpalaikiškumas, kurį lemia perovskitų hidroskopiškumas, todėl antroje šio darbo dalyje buvo susintetinta drėgmei atsparesnė HTM. Įvertinus unikalias fluoro atomo savybes nuspręsta gauti junginius, kurie struktūra būtų panašūs į šiuo metu etaloningais vadinamas medžiagas. Vieną ar kelis vandenilio atomus pakeičiant fluoro atomais buvo išskirtos naujos fluora turinčios organinės molekulės. Nustačius šių medžiagų drėkinimo kampus pastebėta, kad fluoro atomų pridėjimas į molekulę beveik visais atvejais padidina junginių hidrofobiškumą. Remiantis gautais rezultatais galima daryti prielaidą, jog strategiškai fluoro atomų pridėjimas į HTM galėtų pailginti PSC eksploatacijos laiką.

LIST OF ABBREVIATIONS AND PHYSICAL UNITS

δ	chemical shift in parts per million;
μ_0	zero field charge carrier mobility;
μ	charge carrier mobility;
$^1\text{H NMR}$	proton nuclear magnetic resonance;
$^{13}\text{C NMR}$	carbon nuclear magnetic resonance;
CDCl_3	deuterated chloroform;
DMF	<i>N,N</i> -dimethylformamide
DMSO	dimethylsulfoxide;
DSC	differential scanning calorimetry;
FF	fill factor;
FTO	fluorine doped tin oxide;
HOMO	highest occupied molecular orbital;
HTM	hole transporting material;
I_p	ionization potential;
IPCE	incident photon-to-current conversion efficiency;
J	coupling constant in Hz;
J_{sc}	short circuit current-density;
LUMO	lowest unoccupied molecular orbital;
m.p.	melting point;
NBS	N-bromosuccinimide
NMR	nuclear magnetic resonance;
PCE	power conversion efficiency;
ppm	parts per million;
PSC	perovskite solar cell;

RT	room temperature;
Spiro-OMeTAD	2,2',7,7'-tetrakis-(<i>N,N</i> -di- <i>p</i> -methoxyphenylamine)-9,9'-spirobifluorene;
T _{dec}	temperature of 5 % thermal decomposition;
T _g	glass transition temperatures;
TGA	thermogravimetric analysis
T _m	melting point;
THF	tetrahydrofuran;
TLC	thin layer chromatography;
TMS	trimethylsilane;
TPA	triphenylamine;
UV/Vis	ultraviolet/visible;
VBE	valence band energy;
V _{oc}	open circuit voltage;
XTOF	xerographic time of flight technique.

1. INTRODUCTION

Replacement of the imminently depleting fossil fuels by renewable energy sources is possibly the biggest test for humanity. The population also needs to avert the adverse results on health, climate and environment that the present energy system causes. The conditions of peoples lives largely depend on the accessibility to sources of clean energy. It is expected that the amount of energy used will double in the next 30 years [1]. One of the most powerful sources of renewable energy is the sun. 178 TWh of solar energy reaches the surface of the earth each hour, while the annual global demand is 111 TWh. Solar cells are used to convert solar energy into electrical energy. If this technology were to be properly perfected the global demand could be met.

Currently polycrystalline silicon solar cells are the most produced ones and while they generally have good overall performance (~20-25% energy conversion efficiency), they are too expensive due to the difficult technology of silicon purification. In this case, organic compounds provide opportunities to design a much cheaper and simpler solar cell technology.

This work concentrates on the search for alternatives to the best hole transporting material used at this time - 2,2',7,7'-tetrakis-(*N,N*-di-*p*-methoxyphenylamine)-9,9'-spirobifluorene (spiro-OMeTAD).

The aim of this work: to synthesize organic semiconductors containing fluorenyl and carbazolyl chromophores and to investigate the influence of fluoro and methyl groups to these compounds.

Tasks:

1. To synthesize and investigate hole transporting materials containing methyl groups.
2. To synthesize and investigate organic semiconductors containing fluorine atoms.

2. LITERATURE REVIEW

Currently crystalline silicon based solar cells are predominantly used in the world, however their manufacture involves processes which require complex technology and have a high price. One of the few inexpensive substitutes that could be used as an alternative to solar cells based on silicon are organic solar cells.

2.1. Perovskite solar cells

Perovskite solar cells have caused a revolution with their progress in recent years with power conversion efficiencies (PCEs) evolving from 3.8% [2] in 2009 to a certified 22.1% [3] in 2016.

Perovskites are a class of materials with a generic formula ABX_3 . In the formula the anion is X whereas the differently sized cations are B and A, (B being smaller than A). In a cubic structure, they make-up a BX_6 octahedron (**Figure 1**). The cations B are positioned at the center of the octahedron while the anions X are located at the corners. Cations A reside in the gap, surrounded by 8 octahedrons. [4, 5]. Organolead halide perovskites are generally used in PSCs, where typically $A = CH_3NH_3^+$, $B = Pb^{2+}$ and $X = I^-, Br^-, Cl^-$, or mixtures thereof.

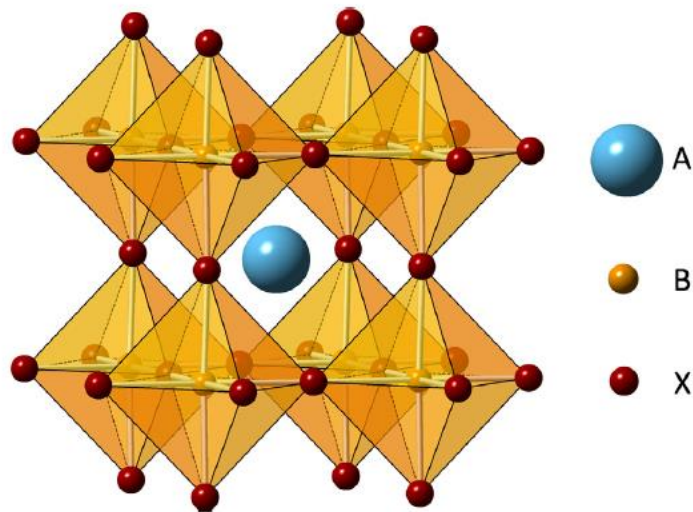


Figure 1. Perovskite ABX_3 crystal structure [6]

PSCs have been traditionally designed with the use of a mesoporous scaffold and a stack architecture (**Figure 2**). The fabrication process of the solar cell begins by forming a compact TiO_2 hole-blocking layer on a fluorine doped tin oxide (FTO) substrate. It is necessary to make the compact

layer homogenous and without pin-holes to avoid recombination between transporters from the FTO and perovskite layers. A mesoporous layer of n-type TiO_2 is formed on the hole-blocking layer by spin coating or screen printing a nanoparticle TiO_2 paste. Annealing is used after for the removal of polymeric binders. The perovskite is then dissolved in a solvent such as N,N-dimethylformamide (DMF) and a layer of it is spin coated on the mesoporous layer. The hole transporting material (with appropriate dopants that improve conductivity) is deposited after that. Lastly, a metal electrode for instance silver (Ag) or gold (Au) is thermally evaporated on the HTM to complete the solar cell [7].

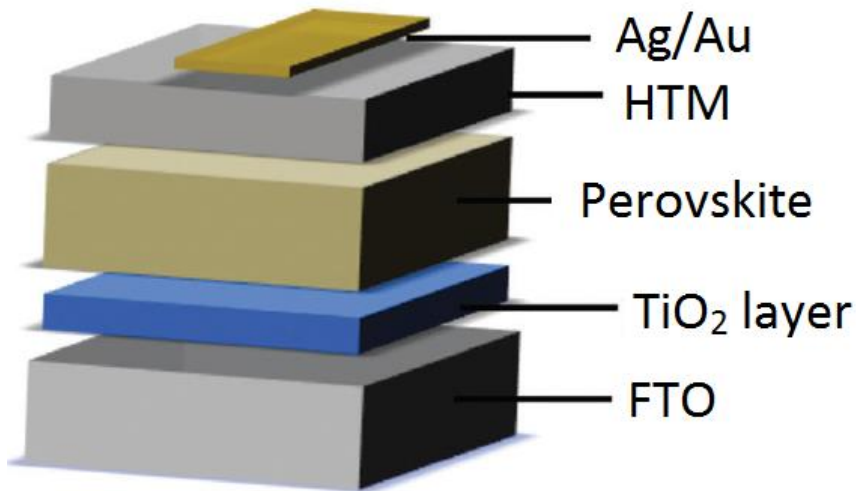
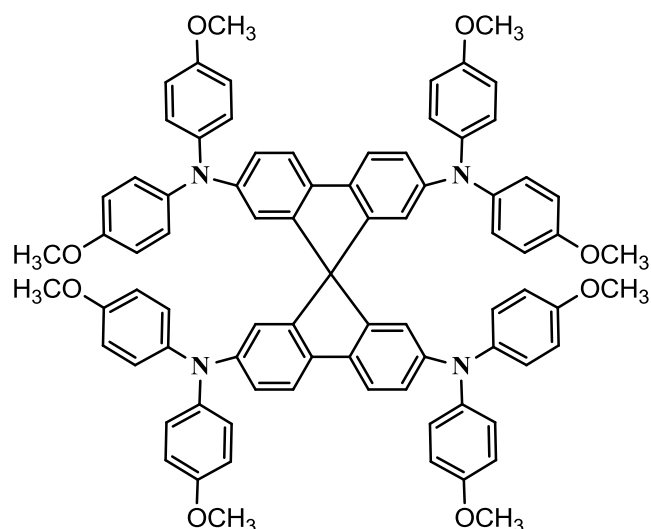


Figure 2. Schematic of a PSC stack [8]

Regardless of the device architecture the HTM layer is one of the key components to prepare highly efficient and stable PSCs [8]. An optimal hole transporting material should meet some general requirements for the PSC to have a higher efficiency, like a compatible HOMO (highest occupied molecular orbital) energy level of the HTM to the valence band energy (VBE) of the perovskite, high photochemical and thermal stability and an ample hole mobility as well [9]. There are four large families of HTMs that can be identified: small molecule, polymeric, carbon and inorganic. The following sections will focus on the influence of methyl and fluorine groups to properties of small molecule HTMs.

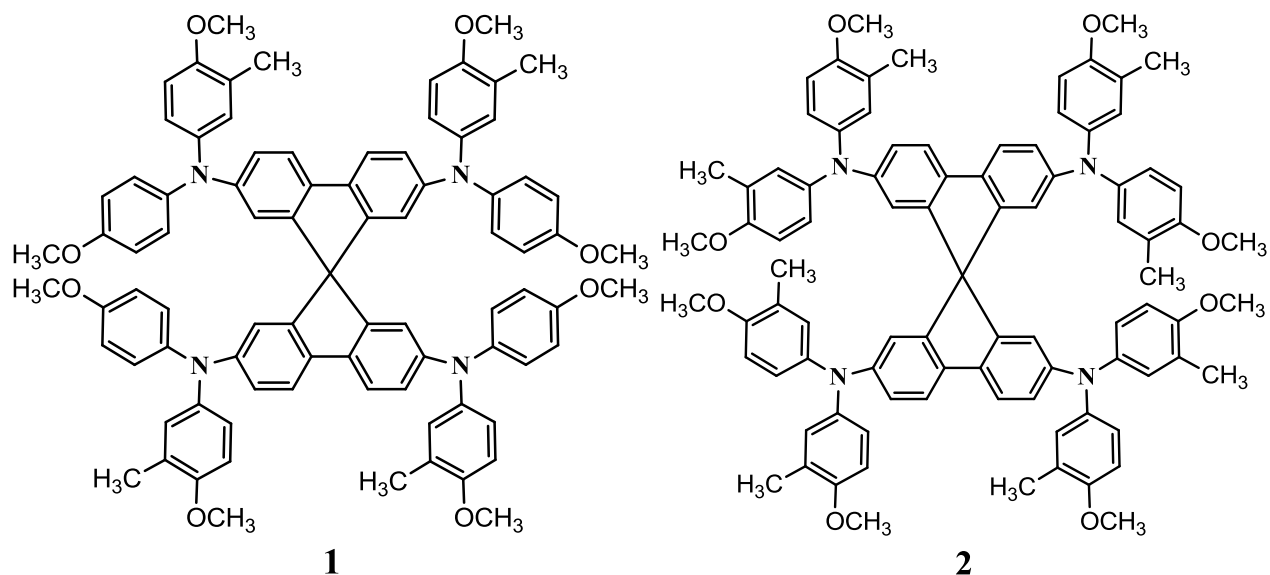
2.2. Properties HTMs containing methyl groups

Compounds based on triphenylamine (TPA) are the best known small molecule HTMs most often used in solar cells. Spiro-OMeTAD is the classic example amidst these hole transporting materials, having been generally used in solar cells [10].

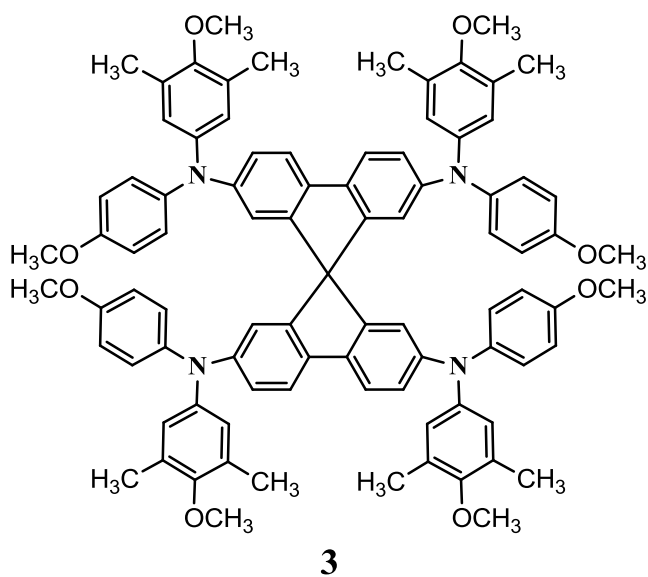


spiro-OMeTAD

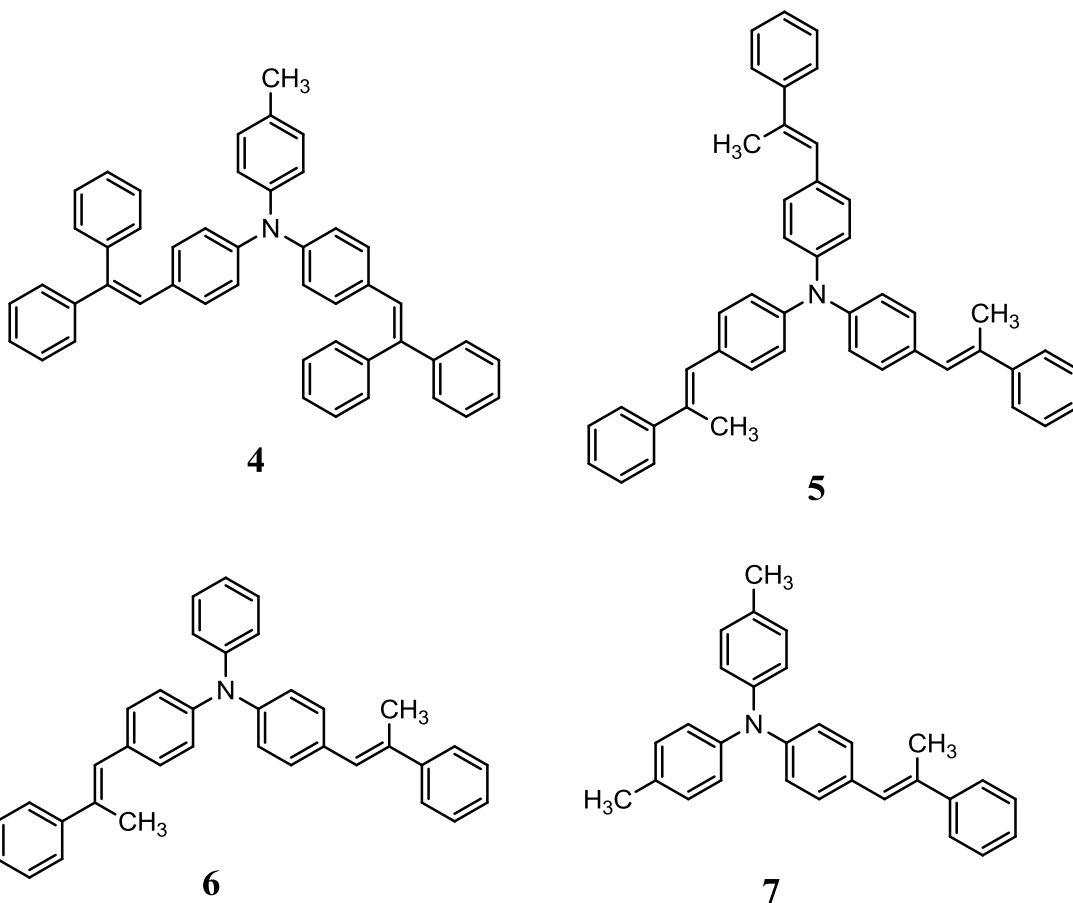
Lukšienė synthesized a series of materials **1-3** which were similar to spiro-OMeTAD but contained methyl groups in different parts of the molecule [11].



Compound **1** had better drift mobility than spiro-OMeTAD, while **2** and **3** showed a slight decrease in that aspect. Solid state dye-sensitized solar cells were constructed using materials **1-3** as HTMs with **1** reaching a PCE of 4.8%, while **2** and **3** both showed PCEs of 2.9%. A device using spiro-OMeTAD was built as a reference and it displayed a 4.8% efficiency demonstrating that more methyl groups in side chains tend to worsen the performance of solar cells.

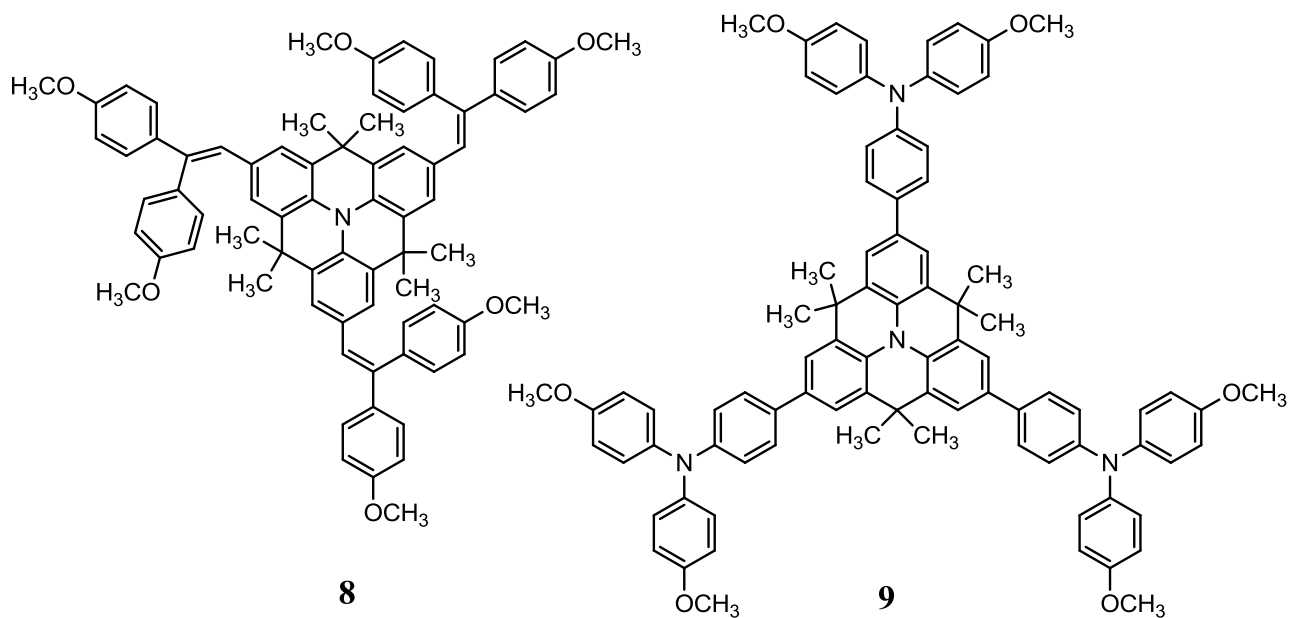


Malinauskas T. *et al.* presented materials **4-7** based on TPA [12].

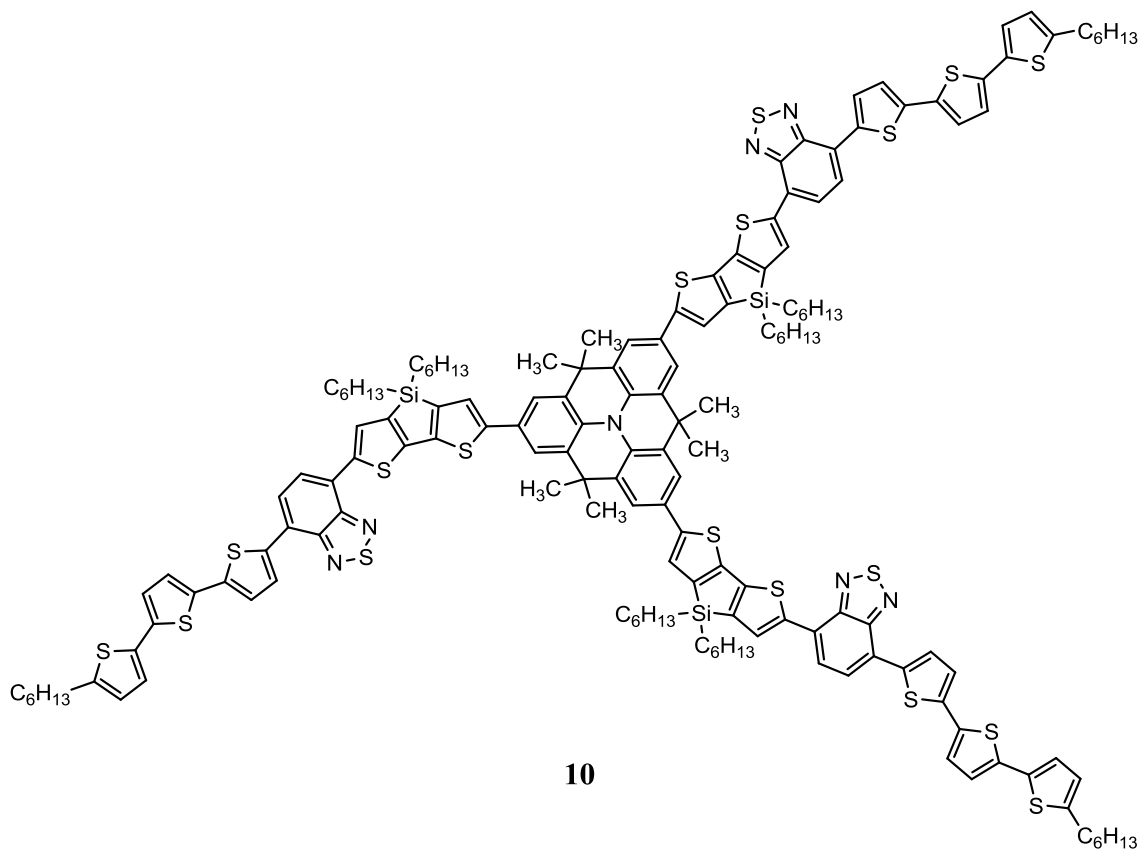


All of the shown compounds have a much higher drift mobility than spiro-OMeTAD and are obtained using a simple one-step synthesis.

Ko and co-workers designed HTMs **8** and **9** incorporating a fused quinolizino arcidine core with methyl groups in the central fragments of the molecules [13, 14].



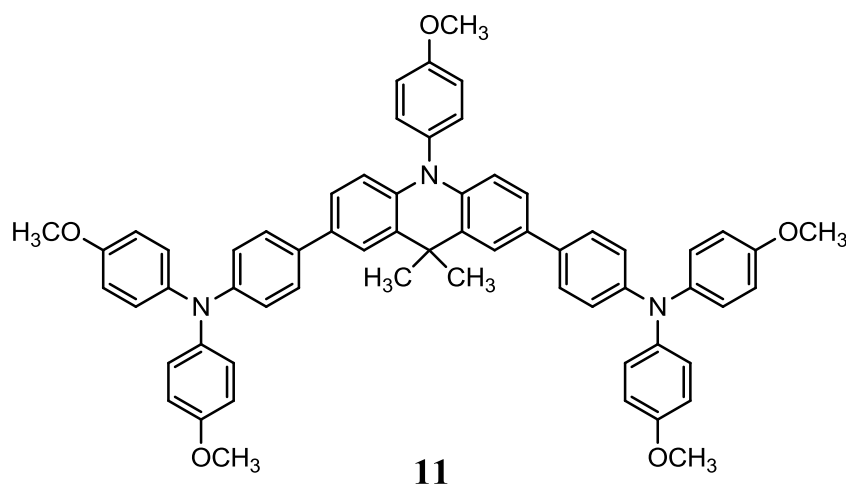
Efficiencies of 11.9% and 13.6% were obtained by using these HTMs in PSCs. Devices with spiro-OMeTAD as a HTM were used as reference and showed PCEs of 12.8% and 14.7% respectively.



Grätzel and Nazeeruddin *et al.* introduced HTM **10** which incorporates a fused quinolizino acridine core also but with side branches based on thiophene [15].

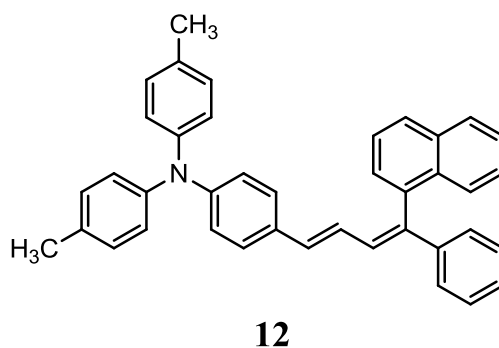
An average efficiency of 12.8% is attained with this HTM, that surpasses the spiro-OMeTAD-based one (11.7%). The PSC with compound **10** shows a much greater incident photon-to-current conversion efficiency (IPCE) than spiro-OMeTAD does in the blue region of the spectra. This suggests that **10** performs as a hole transporting material as well as improves the overall photocurrent.

A. Cho *et al.* presented an acridine-based HTM **11** with two methyl groups at the center of the molecule, obtained through a four step synthesis [16].

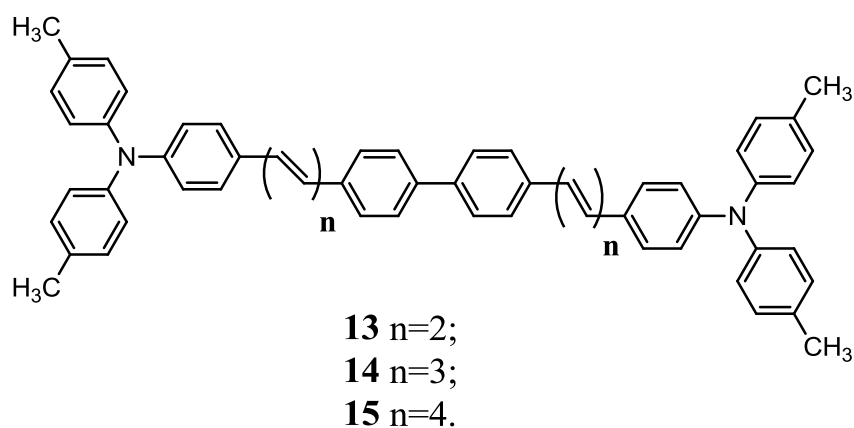


The photovoltaic performance of **11** is comparable to that of spiro-OMeTAD. The PSC based on **11** demonstrates an average PCE of 16.42%, whereas the cell with spiro-OMeTAD shows an average PCE of 16.26%. The synthesis of **11** also is much more cost effective than that of spiro-OMeTAD.

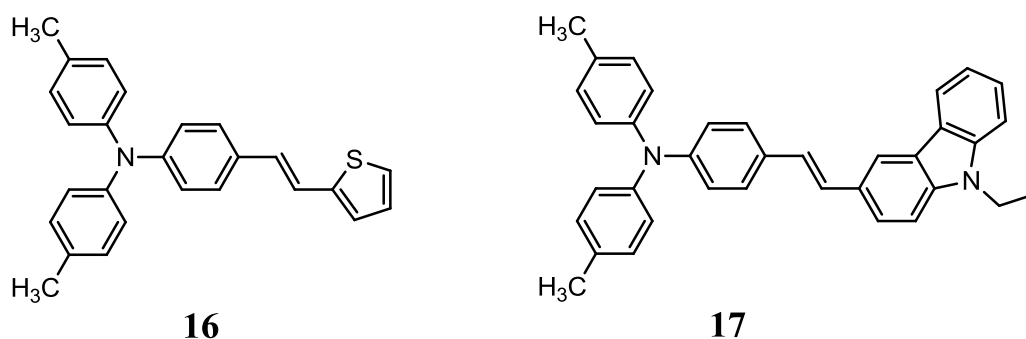
Alternative molecular TPA-based hole transporting materials with methyl groups in different positions have also been produced and displayed acceptable efficiencies. They include a butadiene derivative **12** and π -conjugated linear modified TPA-based compounds **13-15** [17, 18].



HTMs **12-14** exhibit PCE values in the range of 9.1 to 11.3%. Devices using spiro-OMeTAD were also built as reference for each material and displayed efficiencies from 10.2% to 12.1% respectively.

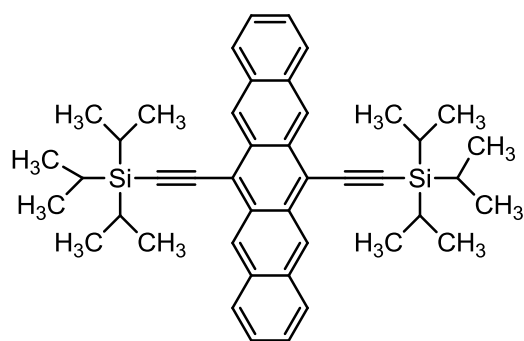


S. Lv *et al.* reported TPA-based materials **16** and **17** containing vinyl derivatives [19].



PSCs were constructed using **16** and **17** as HTMs and the results revealed that **17** exhibited PCEs up to 12%, slightly lower than spiro-OMeTAD (13.1%) under the same fabrication method, whereas **16** had a rather poor performance of 9.0%. One of the contributing factors for such an outcome might have been a rather low hole mobility of material **16**.

S. Kazim *et al.* presented a pentacene based material **18** [20].



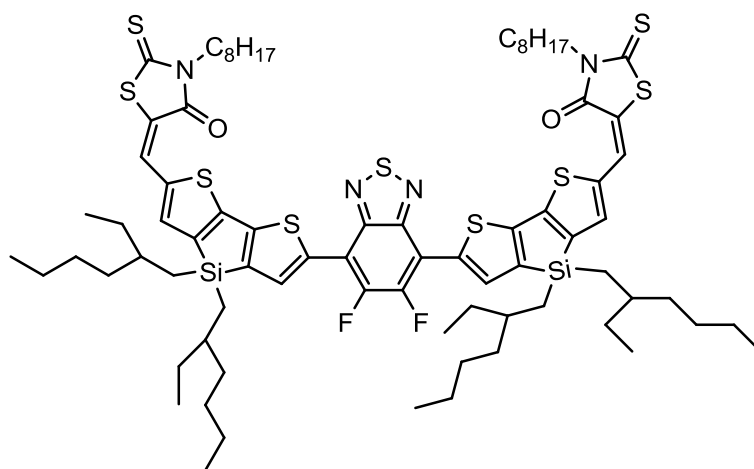
18

It is potentially economical in terms of cost, easily synthesized and shows rather good hole mobility [21, 22]. The device built using **18** as a hole transporting material gave a very competitive performance of 11.8% compared to the classical PSC using spiro-OMeTAD which showed a PCE of 10.1%.

2.3. Properties of HTMs containing fluorine groups

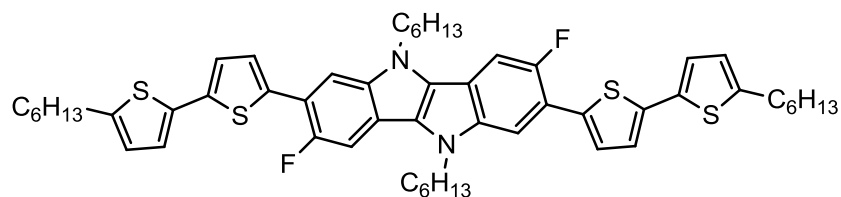
The past decade or two has seen researchers use fluorination as a means to induce stability in organics by lowering both the the lowest unoccupied molecular orbital (LUMO) and HOMO energy levels in the molecule [23].

Y. Liu *et al.* synthesized material **19** containing two fluorine atoms in the central fragment of the molecule [24]. A PSC was constructed using **19** however the device showed an inferior efficiency of 6.2%.



19

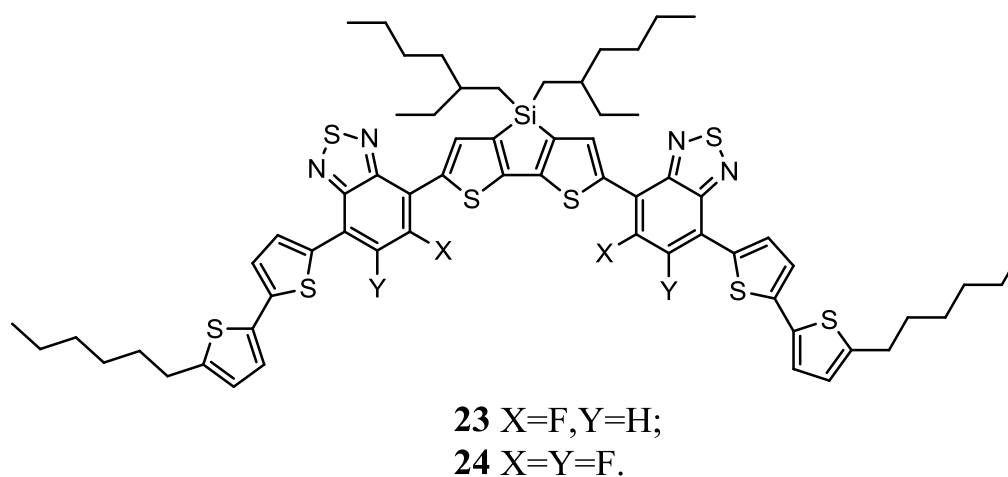
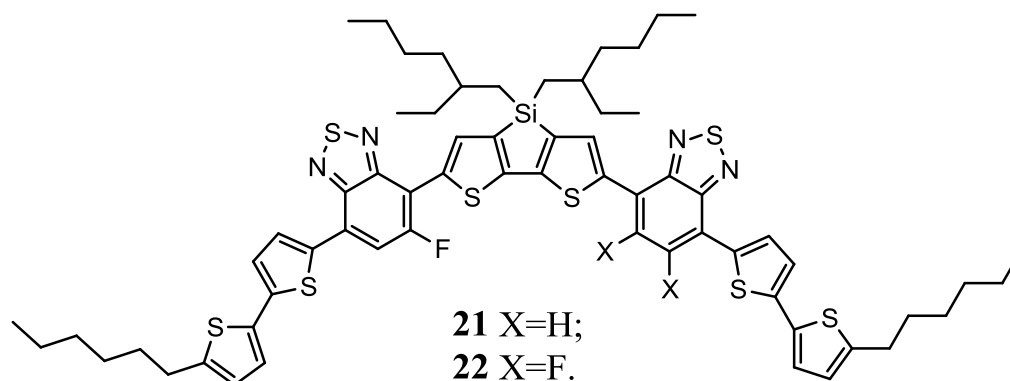
I. Cho *et al.* designed a fluorinated indolo[3,2-b]indole derivative **20** as a crystalline HTM for PSCs [25].



20

Due to the strong π - π interaction between the planar structures of the extended core, **20** shows a higher hole mobility than that of spiro-OMeTAD. The device built using **20** as an HTM displayed an impressive average efficiency of 19.05% proving it to be a promising candidate for highly efficient PSCs.

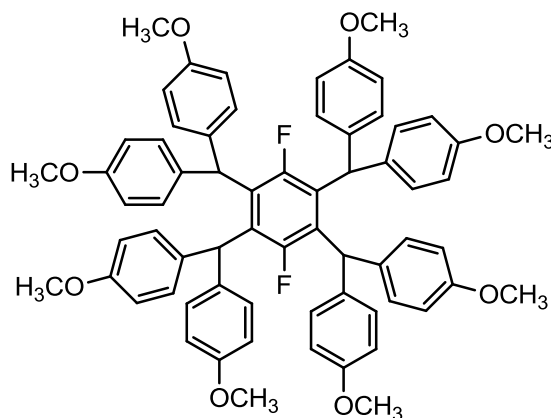
J. H. Yun *et al.* synthesized a series of molecules **21-24** with different fluorine substitution patterns. Depending on symmetricity and the number of fluorine atoms incorporated very different morphological and optical properties can be seen [26].



A similar compound without fluorine atoms was also synthesized as a reference. After hole mobility measurements were done it could be seen that compound **23** exhibited the highest mobility, followed

by compound **24**. Materials **21** and **22** exhibited lower hole mobility values, while the compound that contained no fluorine atoms had the lowest value. This proved that charge transport mobilities were influenced by the symmetry and number of the fluorine atom substitutions. Bulk heterojunction solar cells incorporating materials **21-24** were fabricated and the efficiencies of the cells correlated with the results of hole mobility measurements with **23** showing the highest PCE of 8.14%.

H. Chen *et al.* demonstrated a simple one step synthesis method for HTM **25** [27].



25

The advantages of **25** over spiro-OMeTAD are a simple and cost effective synthesis and a relatively high yield, however PSCs incorporating **25** as a HTM show a PCE of only 10.4% which is significantly lower than the 15% efficiency of equivalent devices fabricated using spiro-OMeTAD [28].

2.4. Literature review conclusions

In recent years perovskite solar cells have experienced an unprecedented rise in PCE and have emerged as a highly efficient photovoltaic technology. Their efficiencies have reached those of their inorganic counterparts and are approaching their practical limitations.

The literature review revealed that there are few simple easily synthesized organic semiconductors that show decent results in PSCs. Most HTMs with strategically placed methyl groups display reasonably good results in perovskite solar cells and are much more cost effective than the conventionally used spiro-OMeTAD. Nonetheless, the influence of fluorine atoms in hole transporting materials has not been studied that extensively. Based on the literature review the search for simple yet effective HTMs should be continued. A broadened sense about the influence of methyl groups and fluorine atoms in organic semiconductors should also be established.

3. MATERIALS AND METHODS

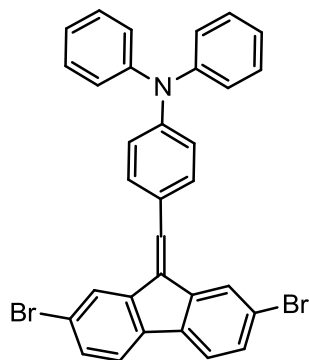
All reagents were purchased from commercial companies and used as received. The ^1H NMR (400 or 700 MHz field strength) and ^{13}C NMR (75 or 176 MHz) spectra were taken on Bruker Avance III 400 (400 MHz) or Bruker Avance III 700 (700MHz) spectrometers at RT. Reactions were magnetically stirred and the course of the reactions products were monitored by TLC on ALUGRAM SIL G/UV254 plates and developed with UV light. Silica gel (grade 9385, 230–400 mesh, 60 Å, Aldrich) was used for column chromatography. The chemical shifts, expressed in ppm, are reported relative to tetramethylsilane (TMS). UV-Vis spectra were recorded on Perkin Elmer Lambda 35 UV/Vis spectrometer. Melting points were determined for crystalline materials on an Electrothermal MEL-TEMP capillary melting point apparatus and are uncorrected. Elemental analysis was performed with an Exeter Analytical CE-440 elemental analyzer, Model 440 C/H/N/. Differential scanning calorimetry was performed on a Q10 calorimeter (TA Instruments) at a scan rate of 10 K min⁻¹ in nitrogen atmosphere. Glass transition temperatures for the synthesized compounds were determined during the second heating cycle Thermogravimetric analysis was performed on a Q50 thermogravimetric analyser (TA Instruments) at a scan rate of 10 K min⁻¹ in the nitrogen atmosphere. The wetting angle was measured with a Theta Lite Optical Tensiometer by the sessile drop measurement method on the HTMs whose solutions were spin coated on a glass substrate.

The solid state ionization potential (I_p) of the layers of the synthesized compounds was measured by the electron photoemission in air method [29]. The hole drift mobility (μ) was measured by xerographic time of flight technique (XTOF) [30]. I_p and μ were measured at the Department of Solid State Electronics, Vilnius University by dr. V. Gaidelis and dr. V. Jankauskas.

3.1. Synthesis of the intermediate compounds

Synthesis of materials **2-4** was described in the Bsc thesis [31].

4-[(2,7-dibromo-9*H*-fluoren-9-ylidene)methyl]-*N,N*-diphenylaniline (1)



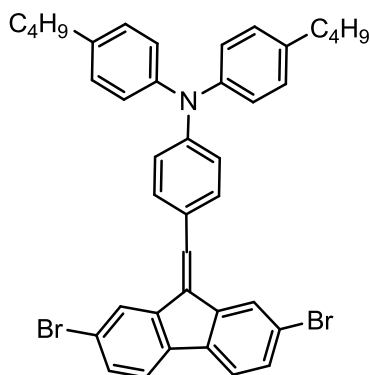
13 ml of 40% NaOH solution and tetrabutylammonium bromide (0.23 g, 0.0072 mol) were added to a solution of 2,7-dibromofluorene (1.3 g 0.004 mol) and 4-(diphenylamino)benzaldehyde (1.09 g, 0.004 mol) in 13 ml of toluene. The reaction was heated at 100 °C for 10 minutes. After cooling, the resulting mixture was quenched with distilled water and extracted with ethyl acetate. The organic layer was dried over anhydrous Na₂SO₄, filtered, and the solvent was evaporated. The crude product was purified by column chromatography using 0.1:24.9 v/v acetone/*n*-hexane as an eluent to collect **1** as an orange solid. Yield 1.97 g (85 %) m.p.: 174–175.5 °C.

¹H NMR (400 MHz, CDCl₃, δ, ppm): 7.87 (dd, *J* = 11.6, 1.5 Hz, 2H), 7.62 (s, 1H), 7.54-7.07 (m, 19H), 1.54 (s, 1H).

¹³C NMR (101 MHz, CDCl₃, δ, ppm): 148.62, 147.18, 141.34, 138.81, 138.16, 136.67, 133.26, 131.07, 130.73, 130.54, 130.21, 129.46, 128.77, 127.27, 125.08, 123.68, 123.44, 122.28, 121.10, 120.97, 120.89, 120.66.

Anal. calcd. for C₃₂H₂₁Br₂N: C, 66.34; H, 3.65; N, 2.42. Found: C, 66.39; H, 3.69; N, 2.22.

4-[(2,7-dibromo-9*H*-fluoren-9-ylidene)methyl]-*N,N*-bis(4-butylphenyl)aniline (5)



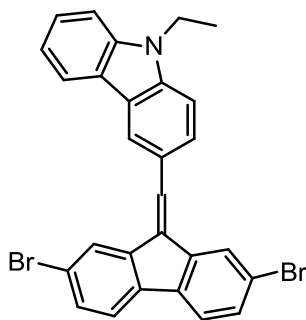
36 ml of 40% NaOH solution and tetrabutylammonium bromide (0.58 g, 0,0018 mol) were added to a solution of 2,7-dibromofluorene (3.24 g 0.01 mol) and 4-[bis(4-butylphenyl)amino]benzaldehyde (3.85 g, 0.01 mol) in 36 ml of toluene. The reaction was heated at 100 °C for 10 minutes. After cooling, the resulting mixture was quenched with distilled water and extracted with ethyl acetate. The organic layer was dried over anhydrous Na₂SO₄, filtered, and the solvent was evaporated. The crude product was purified by column chromatography using 0.1:24.9 v/v acetone/*n*-hexane as an eluent to collect **5** as a orange solid. Yield 5.18 g (75%) m.p.: 75–76.5 °C.

¹H NMR (400 MHz, CDCl₃, δ, ppm): 7.96 (s, 1H), 7.86 (s, 1H), 7.61 (s, 1H), 7.54-7.07 (m, 16H), 2.59 (t, *J* = 7.8 Hz, 4H), 1.60 (quin, *J* = 7.8 Hz, 4H), 1.38 (sex, *J* = 7.8 Hz 4H), 0.95 (t, *J* = 7.8 Hz, 6H).

¹³C NMR (101 MHz, CDCl₃, δ, ppm): 149.09, 144.70, 141.49, 138.72, 138.57, 138.22, 136.55, 132.67, 130.93, 130.55, 129.37, 127.64, 127.20, 125.27, 123.36, 121.05, 120.93, 120.85, 120.64, 35.12, 33.67, 22.45, 14.00.

Anal. calcd. for C₄₀H₃₇Br₂N: C, 69.47; H, 5.39; N, 2.03. Found: C, 69.40; H, 5.43; N, 2.09.

3-[(2,7-dibromo-9H-fluoren-9-ylidene)methyl]-9-ethyl-9H-carbazole (**6**)



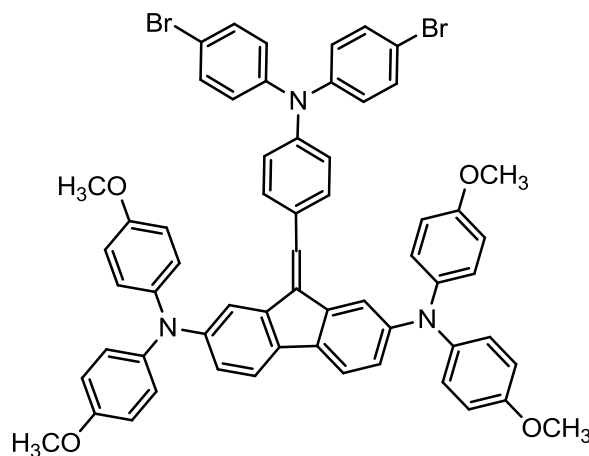
15 ml of 40% NaOH solution and tetrabutylammonium bromide (0.29 g, 0,0009 mol) were added to a solution of 2,7-dibromofluorene (1.62 g 0.005 mol) and 9-ethyl-3-carbazolcarboxyaldehyde (1.11 g, 0.005 mol) in 15 ml of toluene. The reaction was heated at 100 °C for 10 minutes. After cooling, the resulting mixture was quenched with distilled water and extracted with ethyl acetate. The organic layer was dried over anhydrous Na₂SO₄, filtered, and the solvent was evaporated. The crude product was purified by column chromatography using 1:24 v/v tetrahydrofuran/*n*-hexane as an eluent to collect **6** as a yellow solid. Yield 1.5 g (57 %) m.p.: 172–174°C.

^1H NMR (400 MHz, CDCl_3 , δ , ppm): 8.27 (s, 1H), 8.04-7.17 (m, 13H), 4.33 (q, $J = 7.2$ Hz, 2H), 1.42 (t, $J = 7.8$ Hz, 3H).

^{13}C NMR (101 MHz, CDCl_3 , δ , ppm): 141.70, 140.47, 140.25, 138.82, 138.33, 136.53, 132.31, 131.93, 131.04, 130.51, 127.66, 126.84, 126.25, 125.95, 123.38, 123.25, 122.88, 122.01, 121.09, 120.98, 120.88, 120.69, 120.60, 119.57, 108.84, 108.57, 37.82, 13.91.

Anal. calcd. for $\text{C}_{28}\text{H}_{19}\text{Br}_2\text{N}$: C, 63.54; H, 3.62; N, 2.65. Found: C, 63.70; H, 3.69; N, 2.43.

4-[[2,7-bis(4,4'-dimethoxydiphenylamino)-9H-fluoren-9-ylidene]methyl]-N,N-bis(4-bromophenyl)aniline (7)



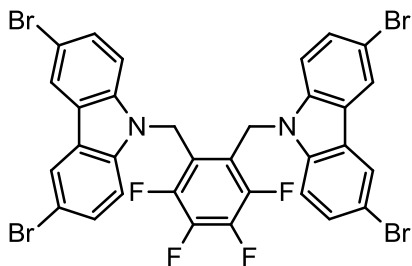
A solution of N-bromosuccinimide (NBS) (0.4g 0.0023mol) in dimethylformamide (DMF) (10 ml) was added dropwise over 30 min to a stirred solution of **HTM1** (1g 0.0011 mol) in DMF (10 ml) at 0 °C. The resulting solution continued to be stirred at 0 °C for 6 h. The resulting mixture was quenched with distilled water and extracted with ethyl acetate. The organic layer was dried over anhydrous Na_2SO_4 , filtered, and the solvent was evaporated. The crude product was purified by column chromatography using 2.5:22.5 v/v acetone/*n*-hexane as an eluent to collect **7** as a red solid. Yield 0.57 g (50%) m.p.: 120–122 °C.

^1H NMR (400 MHz, CDCl_3 , δ , ppm): 7.51 (s, 1H), 7.71-7.41 (m, 36H), 3.79 (s, 6H), 3.63 (s, 6H).

^{13}C NMR (101 MHz, CDCl_3 , δ , ppm): 147.04, 146.78, 146.66, 132.17, 130.39, 129.39, 129.22, 125.26, 124.52, 124.26, 123.94, 123.42, 119.37, 114.63, 55.50, 55.37, 29.70.

Anal. calcd. for C₆₀H₄₇Br₂N₃O₄: C, 69.71; H, 4.58; N, 4.06. Found: C, 69.60; H, 4.63; N, 4.22.

1,2-Bis(3,6-dibromo-9H-carbazol-9-methyl)-3,4,5,6-tetrafluorobenzene (8)



A mixture of 3,6-dibromo-9H-carbazole (0.98 g, 0,003 mol) and 3,4,5,6-Tetrafluoro-o-xylylene dibromide (0.5 g, 0,0015 mol) was dissolved in 20 ml of dioxane and 0.59 g (0.009 mol) of 85% powdered potassium hydroxide was added in small portions during 2-3 minutes. The obtained mixture was stirred at room temperature for 30 min. The product was filtered off and washed with water until neutral to collect **8** as a white solid. Yield 0.99 g (80%) m.p.: 324–326 °C.

¹H NMR (400 MHz, CDCl₃, δ, ppm): 8.45 (s, 4H), 7.69-7.24 (m, 9H), 6.02 (s, 3H).

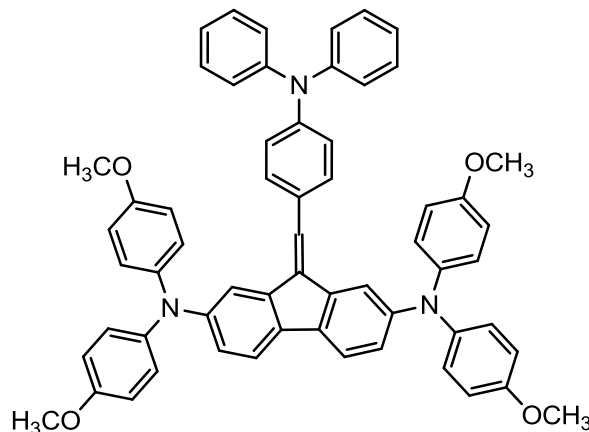
¹³C NMR (101 MHz, CDCl₃, δ, ppm): 139.50, 133.91, 129.51, 123.98, 123.77, 112.45, 112.16.

Anal. calcd. for C₃₂H₁₆Br₄F₄N₂: C, 46.64; H, 1.96; N, 3.40. Found: C, 46.72; H, 1.85; N, 3.43.

3.2. Synthesis of HTMs

Synthesis of materials **HTM2-4** was described in the Bsc thesis [31].

4-[[2,7-bis(4,4'-dimethoxydiphenylamino)-9H-fluoren-9-ylidene]methyl]-N,N-bis(4,4'-dibromodiphenyl)-aniline (HTM1)



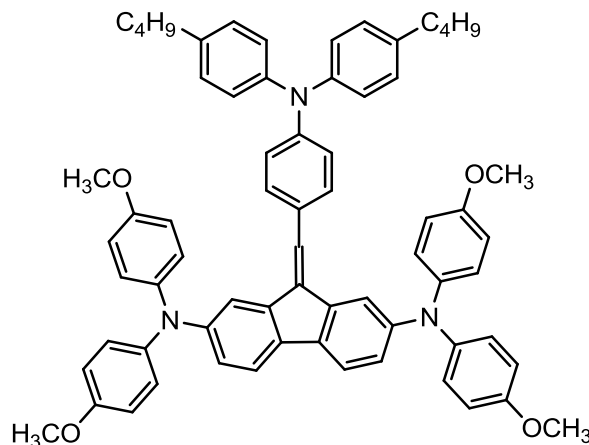
The mixture of **1** (1.16 g, 0.002 mol), bis(4-methoxyphenyl)amine (1.38 g, 0.006 mol), palladium acetate (0.009 g, 0.00004 mol), tri-tert-butylphosphonium tetrafluoroborate (0.016 g, 0.000054 mol), sodium tert-butoxide (0.58 g, 0.006 mol) in 13 ml of anhydrous toluene was refluxed for 52 hours under argon atmosphere. Afterwards, water was added and the extraction was done with ethyl acetate. The organic layer was dried over anhydrous Na₂SO₄, filtered, and the solvent was evaporated. The crude product was purified by column chromatography using 1:24 v/v tetrahydrofuran/*n*-hexane as an eluent to **HTM1** as a orange solid. The 20% solution of the solid residue in acetone was poured while intensively stirring into a twentyfold excess of ethanol. Yield: 1.40 g (80%).

¹H NMR (400 MHz, CDCl₃, δ ppm): 7.40-6.71 (m, 37H), 3.79 (s, 6H), 3.61 (s, 6H).

¹³C NMR (101 MHz, CDCl₃, δ ppm): 147.65, 147.49, 141.10, 130.44, 129.36, 124.41, 123.90, 123.01, 119.57, 114.73, , 55.63, 55.52.

Anal. calcd. for C₆₀H₄₉N₃O₄: C, 82.26; H, 5.64; N, 4.80. Found: C, 82.27; H, 5.60; N, 4.77.

4-[[2,7-bis(4,4'-dimethoxydiphenylamino)-9H-fluoren-9-ylidene]methyl]-N,N-bis(4-butylphenyl)aniline (HTM5)



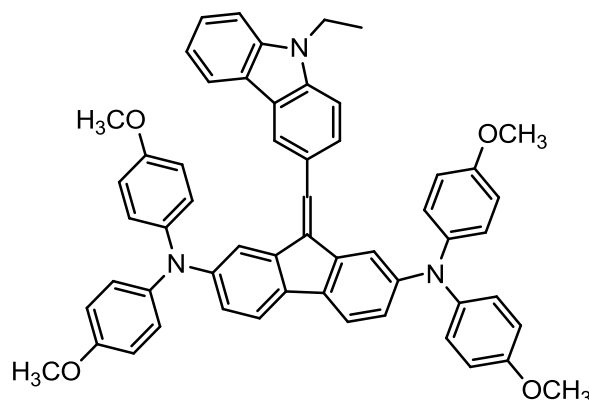
The mixture of **5** (1.38 g, 0.002 mol), bis(4-methoxyphenyl)amine (1.38 g, 0.006 mol), palladium acetate (0.009 g, 0.00004 mol), tri-tert-butylphosphonium tetrafluoroborate (0.016 g, 0.000054 mol), sodium tert-butoxide (0.58 g, 0.006 mol) in 14 ml of anhydrous toluene was refluxed for 52 hours under argon atmosphere. Afterwards, water was added and the extraction was done with ethyl acetate. The organic layer was dried over anhydrous Na₂SO₄, filtered, and the solvent was evaporated. The crude product was purified by column chromatography using 1:24 v/v tetrahydrofuran/*n*-hexane as an eluent to collect **HTM5** as a red solid. The 20% solution of the solid residue in acetone was poured while intensively stirring into a twentyfold excess of ethanol. Yield: 0.99 g (50%).

¹H NMR (400 MHz, CDCl₃, δ, ppm): 7.56-6.71 (m, 35H), 3.79 (s, 6H), 3.62 (s, 6H), 2.56 (t, *J* = 15.5 Hz, 4H), 1.59 (quin, *J* = 15.5 Hz, 4H), 1.38 (sex, *J* = 15.5 Hz, 4H), 0.94 (t, *J* = 7.3 Hz, 6H).

¹³C NMR (101 MHz, CDCl₃, δ, ppm): 147.82, 145.20, 137.55, 130.19, 129.39, 129.10, 124.36, 122.77, 119.48, 114.53, 55.50, 55.37, 35.07, 33.71, 22.46, 14.00.

Anal. calcd. for C₆₈H₆₅N₃O₄: C, 82.64; H, 6.63; N, 4.25. Found: C, 82.42; H, 6.65; N, 4.35.

3-[[2,7--bis(4,4'-dimethoxydiphenylamino)-9H-fluoren-9-ylidene]methyl]-9-ethyl-9H-carbazole (HTM6)



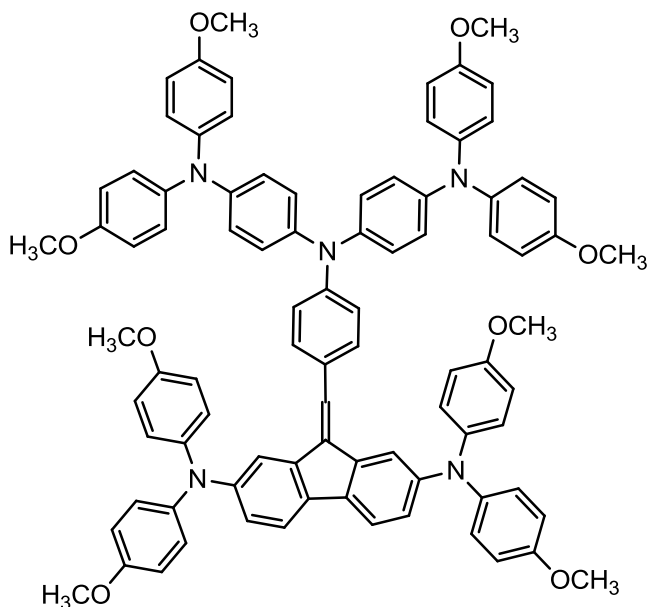
The mixture of **7** (0.53 g, 0.001 mol), bis(4-methoxyphenyl)amine (0.69 g, 0.003 mol), palladium acetate (0.0045 g, 0.00002 mol), tri-tert-butylphosphonium tetrafluoroborate (0.008 g, 0.000027 mol), sodium tert-butoxide (0.29 g, 0.003 mol) in 6 ml of anhydrous toluene was refluxed for 48 hours under argon atmosphere. Afterwards, water was added and the extraction was done with ethyl acetate. The organic layer was dried over anhydrous Na₂SO₄, filtered, and the solvent was evaporated. The crude product was purified by column chromatography using 2.5:22.5 v/v acetone/*n*-hexane as an eluent to collect **HTM6** as a orange solid. The 20% solution of the solid residue in acetone was poured while intensively stirring into a twentyfold excess of methanol. Yield: 0.83 g (62%).

¹H NMR (400 MHz, CDCl₃, δ, ppm): 8.00 (s, 1H), 7.90-6.59 (m, 28H), 4.22 (q, *J* = 7.2 Hz, 2H), 3.72 (s, 6H), 3.62 (s, 6H), 1.33 (t, *J* = 7.8 Hz, 3H).

¹³C NMR (101 MHz, CDCl₃, δ, ppm): 140.26, 139.59, 127.12, 125.80, 122.91, 122.82, 120.51, 119.13, 108.60, 107.88, 55.53, 55.40, 37.53, 13.84.

Anal. calcd. for C₅₆H₄₇N₃O₄: C, 81.43; H, 5.74; N, 5.09. Found: C, 81.50; H, 5.69; N, 5.21.

4-[[2,7-bis(4,4'-dimethoxydiphenylamino)-9H-fluoren-9-ylidene]methyl)-N,N-bis(4,4'-dimethoxydiphenylamino)phenyl)aniline (HTM7)



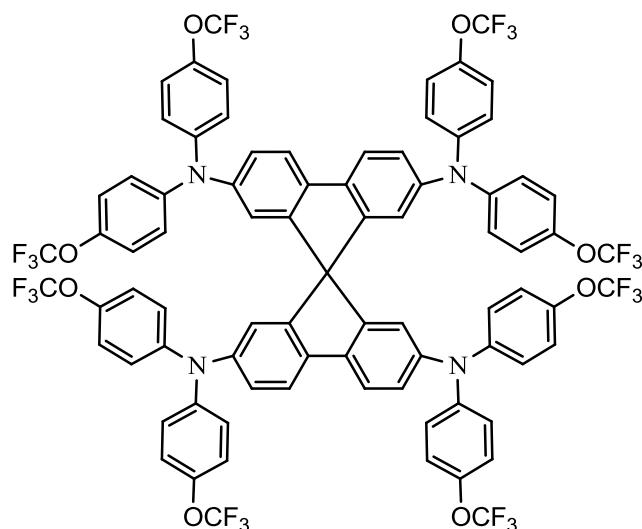
The mixture of **6** (0.83 g, 0.0008 mol), bis(4-methoxyphenyl)amine (0.55 g, 0.0024 mol), palladium acetate (0.004 g, 0.000016 mol), tri-tert-butylphosphonium tetrafluoroborate (0.006 g, 0.0000216 mol), sodium tert-butoxide (0.23 g, 0.0024 mol) in 7 ml of anhydrous toluene was refluxed for 24 hours under argon atmosphere. Afterwards, water was added and the extraction was done with ethyl acetate. The organic layer was dried over anhydrous Na₂SO₄, filtered, and the solvent was evaporated. The crude product was purified by column chromatography using 3:22 v/v acetone/*n*-hexane as an eluent to collect **HTM7** as a red solid. The 20% solution of the solid residue in tetrahydrofurane was poured while intensively stirring into a twentyfold excess of ethanol. Yield: 0.66 g (61%).

¹H NMR (400 MHz, CDCl₃, δ, ppm): 7.44-6.75 (m, 51H), 3.83 (s, 14H), 3.66 (s, 7H).

¹³C NMR (101 MHz, CDCl₃, δ, ppm): 114.57, 55.52, 55.41.

Anal. calcd. for C₈₈H₇₅N₅O₈: C, 79.44; H, 5.68; N, 5.26. Found: C, 79.33; H, 5.82; N, 5.30.

2,2',7,7'-Tetrakis[4,4'-bis(trifluoromethoxy)diphenylamino]-9,9'-spirobifluorene (HTM8)



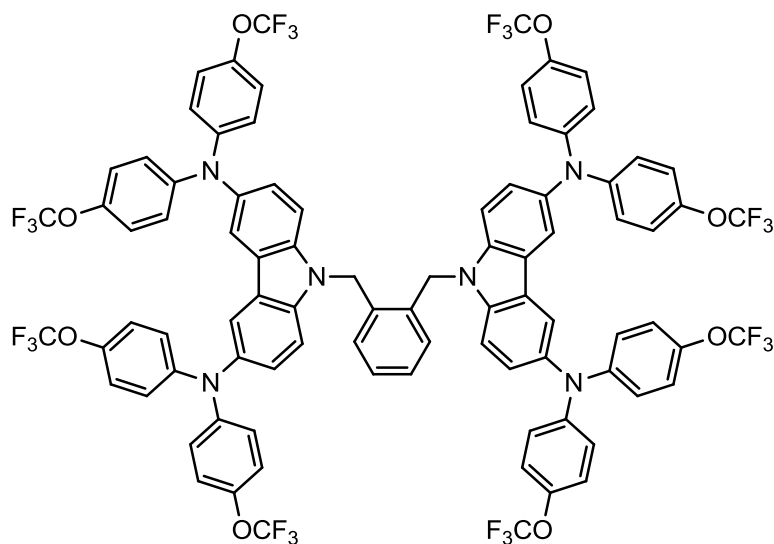
The mixture of 2,2',7,7'-tetrabromo-9,9'-spirobifluorene (0.63 g, 0.001 mol), bis(4-(trifluoromethoxy)phenyl)amine (1.69 g, 0.005 mol), palladium acetate (0.0045 g, 0.00002 mol), tri-tert-butylphosphonium tetrafluoroborate (0.008 g, 0.000027 mol), sodium tert-butoxide (0.48 g, 0.005 mol) in 12 ml of anhydrous toluene was refluxed for 24 hours under argon atmosphere. Afterwards, water was added and the extraction was done with ethyl acetate. The organic layer was dried over anhydrous Na_2SO_4 , filtered, and the solvent was evaporated. The crude product was purified by column chromatography using *n*-hexane as an eluent to collect **HTM8** as a white solid.. Yield: 1.38 g (83%).

^1H NMR (400 MHz, CDCl_3 , δ , ppm): 7.57 (d, $J = 8.2$ Hz, 4H), 7.06-6.93 (m, 36H), 6.59 (s, 4H).

^{13}C NMR (101 MHz, CDCl_3 , δ , ppm): 150.03, 146.42, 145.97, 144.28, 137.23, 125.56, 124.34, 123.98, 122.14, 121.79, 121.14, 120.32, 119.24, 116.68, 65.50.

Anal. calcd. for $\text{C}_{81}\text{H}_{44}\text{F}_{24}\text{N}_4\text{O}_8$: C, 74.56; H, 5.12; N, 5.93. Found: C, 74.62; H, 5.09; N, 5.86.

**1,2-Bis[3,6-{4,4'-bis(trifluoromethoxy)diphenylamino}-9H-carbazol-9-methyl]benzene
(HTM9)**



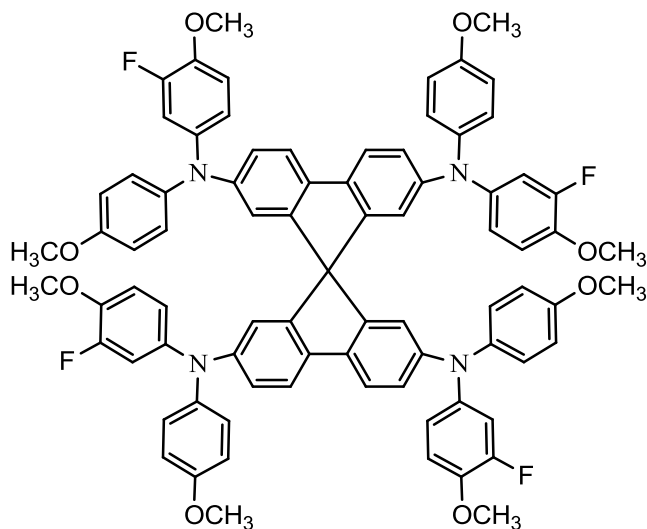
The mixture of 1,2-Bis(3,6-dibromo-9H-carbazol-9-methyl)benzene (0.75 g, 0.001 mol), bis(4-(trifluoromethoxy)phenyl)amine (1.69 g, 0.005 mol), palladium acetate (0.0045 g, 0.00002 mol), tri-tert-butylphosphonium tetrafluoroborate (0.008 g, 0.000027 mol), sodium tert-butoxide (0.48 g, 0.005 mol) in 12 ml of anhydrous toluene was refluxed for 70 hours under argon atmosphere. Afterwards, water was added and the extraction was done with ethyl acetate. The organic layer was dried over anhydrous Na₂SO₄, filtered, and the solvent was evaporated. The crude product was purified by column chromatography using 1:24 v/v acetone/*n*-hexane as an eluent to collect **HTM9** as a yellow solid. Yield: 1.21 g (69%).

¹H NMR (700 MHz, CDCl₃, δ, ppm): 7.81 (s, 4H), 7.24-6.95 (m, 44H), 5.54 (s, 4H).

¹³C NMR (176 MHz, CDCl₃, δ, ppm): 146.76, 143.76, 139.66, 138.67, 133.57, 128.50, 127.25, 126.10, 123.90, 123.38, 122.72, 122.11, 121.27, 119.81, 119.19, 118.35, 110.30, 45.08.

Anal. calcd. for C₈₈H₅₂F₂₄N₆O₈: C, 59.47; H, 2.95; N, 4.73. Found: C, 59.53; H, 3.01; N, 4.72.

**2,2',7,7'-Tetrakis[3-fluoro-4-methoxy-N-(4-methoxyphenyl)anilino]-9,9'-spirobifluorene
(HTM10)**



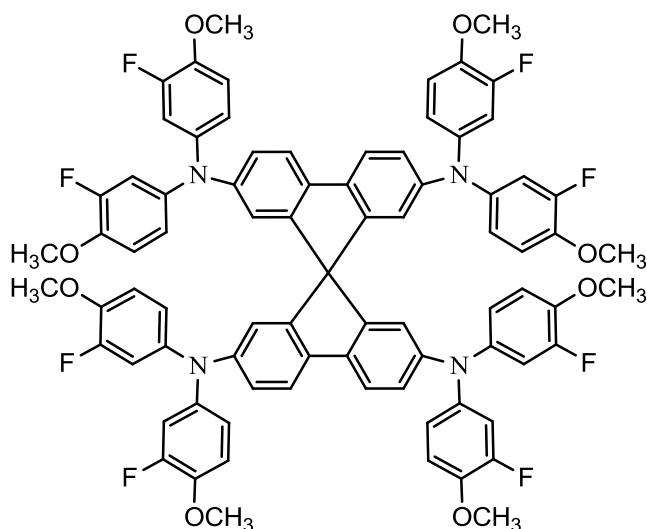
The mixture of 2,2',7,7'-tetrabromo-9,9'-spirobifluorene (0.63 g, 0.001 mol), 3-fluoro-4-methoxy-N-(4-methoxyphenyl)aniline (1.23 g, 0.005 mol), palladium acetate (0.0045 g, 0.00002 mol), tri-tert-butylphosphonium tetrafluoroborate (0.008 g, 0.000027 mol), sodium tert-butoxide (0.48 g, 0.005 mol) in 9 ml of anhydrous toluene was refluxed for 36 hours under argon atmosphere. Afterwards, water was added and the extraction was done with ethyl acetate. The organic layer was dried over anhydrous Na_2SO_4 , filtered, and the solvent was evaporated. The crude product was purified by column chromatography using 3:22 v/v acetone/*n*-hexane as an eluent to collect **HTM10** as a white solid. The 20% solution of the solid residue in tetrahydrofuran was poured while intensively stirring into a twentyfold excess of methanol. Yield: 1.08 g (84%).

^1H NMR (700 MHz, CDCl_3 , δ , ppm): 7.43 (s, 4H), 6.93-6.55 (m, 36H), 3.87 (s, 12H), 3.81 (s, 12H).

^{13}C NMR (176 MHz, CDCl_3 , δ , ppm): 149.99, 118.25, 114.64, 56.80, 55.49.

Anal. calcd. for $\text{C}_{81}\text{H}_{64}\text{F}_4\text{N}_4\text{O}_8$: C, 74.99; H, 4.97; N, 4.32. Found: C, 75.01; H, 5.09; N, 4.23.

2,2',7,7'-Tetrakis[bis(3-fluoro-4-methoxyphenyl)amine]-9,9'-spirobifluorene (HTM11)



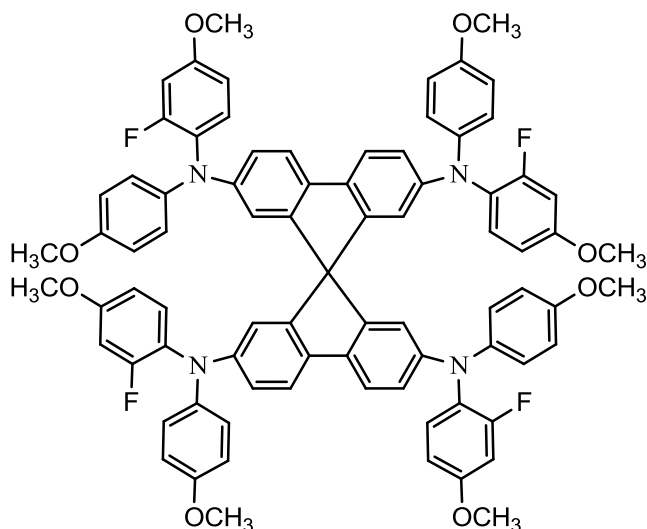
The mixture of 2,2',7,7'-tetrabromo-9,9'-spirobifluorene (1.26 g, 0.002 mol), bis(3-fluoro-4-methoxyphenyl)amine (2.65 g, 0.01 mol), palladium acetate (0.009 g, 0.00004 mol), tri-tert-butylphosphonium tetrafluoroborate (0.016 g, 0.000054 mol), sodium tert-butoxide (0.96 g, 0.01 mol) in 19.5 ml of anhydrous toluene was refluxed for 46 hours under argon atmosphere. Afterwards, water was added and the extraction was done with ethyl acetate. The organic layer was dried over anhydrous Na_2SO_4 , filtered, and the solvent was evaporated. The crude product was purified by column chromatography using 2:3 v/v tetrahydrofuran/*n*-hexane as an eluent to collect **HTM11** as a white solid. The 20% solution of the solid residue in tetrahydrofuran was poured while intensively stirring into a twentyfold excess of *n*-hexane. Yield: 2.05 g (75%).

^1H NMR (700 MHz, DMSO, δ , ppm): 7.56 (d, $J = 8.3$ Hz, 4H), 7.01 (t, $J = 8.3$ Hz, 8H) 6.78-6.65 (m, 20H), 3.78 (s, 24H).

^{13}C NMR (176 MHz, DMSO, δ , ppm): 152.72, 151.33, 149.74, 146.78, 143.94, 143.88, 140.51, 140.46, 135.27, 122.27, 121.26, 120.78, 116.62, 115.04, 112.67, 112.56, 65.47, 56.57.

Anal. calcd. for $\text{C}_{81}\text{H}_{60}\text{F}_8\text{N}_4\text{O}_8$: C, 71.05; H, 4.42; N, 4.09. Found: C, 71.00; H, 4.31; N, 4.12.

**2,2',7,7'-Tetrakis[2-fluoro-4-methoxy-N-(4-methoxyphenyl)anilino]-9,9'-spirobifluorene
(HTM12)**



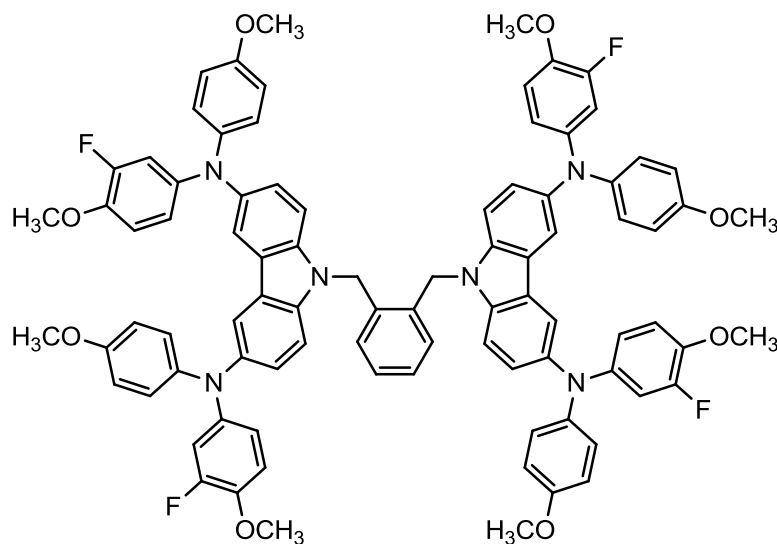
The mixture of 2,2',7,7'-tetrabromo-9,9'-spirobifluorene (0.63 g, 0.001 mol), 2-fluoro-4-methoxy-N-(4-methoxyphenyl)aniline (1.23 g, 0.005 mol), palladium acetate (0.0045 g, 0.00002 mol), tri-tert-butylphosphonium tetrafluoroborate (0.008 g, 0.000027 mol), sodium tert-butoxide (0.48 g, 0.005 mol) in 9 ml of anhydrous toluene was refluxed for 96 hours under argon atmosphere. Afterwards, water was added and the extraction was done with ethyl acetate. The organic layer was dried over anhydrous Na₂SO₄, filtered, and the solvent was evaporated. The crude product was purified by column chromatography using 2:3 v/v tetrahydrofuran/*n*-hexane as an eluent to collect **HTM12** as a white solid. The 20% solution of the solid residue in tetrahydrofuran was poured while intensively stirring into a twentyfold excess of *n*-hexane. Yield: 0.66 g (51%).

¹H NMR (400 MHz, CDCl₃, δ, ppm): 7.24-6.62 (m, 36H), 3.77 (s, 24H).

¹³C NMR (176 MHz, CDCl₃, δ, ppm): 149.99, 118.25, 114.64, 56.80, 55.49.

Anal. calcd. for C₈₁H₆₄F₄N₄O₈: C, 74.99; H, 4.97; N, 4.32. Found: C, 74.87; H, 4.90; N, 4.33.

1,2-Bis[3,6-{3-fluoro-4-methoxy-N-(4-methoxyphenyl)anilino}-9H-carbazol-9-methyl]benzene (HTM13)



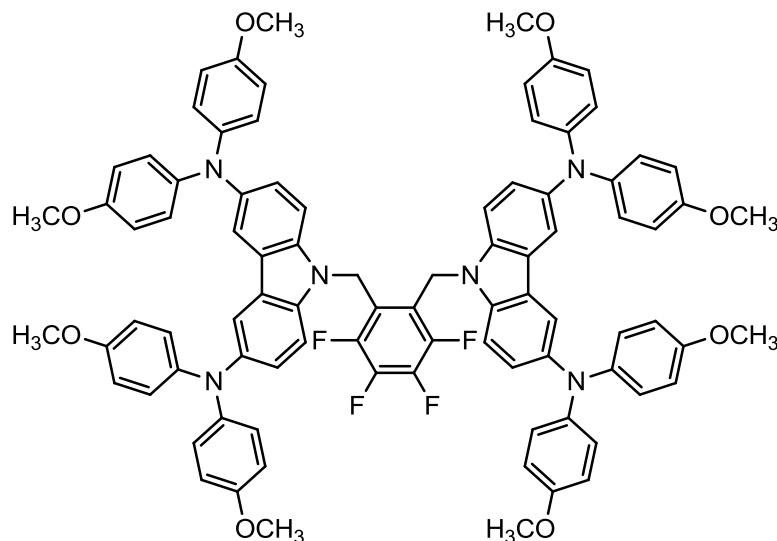
The mixture of 1,2-Bis(3,6-dibromo-9H-carbazol-9-methyl)benzene (0.75 g, 0.001 mol), 3-fluoro-4-methoxy-N-(4-methoxyphenyl)anilino (1.23 g, 0.005 mol), palladium acetate (0.0045 g, 0.00002 mol), tri-tert-butylphosphonium tetrafluoroborate (0.008 g, 0.000027 mol), sodium tert-butoxide (0.48 g, 0.005 mol) in 10 ml of anhydrous toluene was refluxed for 72 hours under argon atmosphere. Afterwards, water was added and the extraction was done with ethyl acetate. The organic layer was dried over anhydrous Na₂SO₄, filtered, and the solvent was evaporated. The crude product was purified by column chromatography using 6:19 v/v acetone/*n*-hexane as an eluent to collect **HTM13** as a yellow solid. The 20% solution of the solid residue in tetrahydrofuran was poured while intensively stirring into a twentyfold excess of methanol. Yield: 1.16 g (82%).

¹H NMR (700 MHz, CDCl₃, δ, ppm): 7.68 (s, 4H), 7.20 (d, *J* = 9.0 Hz, 2H), 7.13 (dd, *J* = 8.7, 2.0 Hz, 4H), 7.04 (d, *J* = 8.7 Hz, 4H), 7.00 (d, *J* = 8.9 Hz, 8H), 6.93 (dd, *J* = 5.3, 3.6 Hz, 2H), 6.79-6.66 (m, 20H) 5.46 (s, 4H), 3.82 (s, 12H), 3.76 (s, 12H).

¹³C NMR (176 MHz, CDCl₃, δ, ppm): 155.41, 153.46, 152.07, 143.37, 143.33, 142.06, 142.00, 141.56, 140.59, 137.86, 133.93, 128.24, 127.24, 125.52, 124.80, 123.70, 117.40, 117.04, 114.70, 114.49, 110.37, 110.26, 109.76, 56.90, 55.49, 45.01.

Anal. calcd. for C₈₈H₇₂F₄N₆O₈: C, 74.56; H, 5.12; N, 5.93. Found: C, 74.62; H, 5.08; N, 5.94.

1,2-Bis[3,6-(4,4'-dimethyldiphenylamino)-9H-carbazol-9-methyl]-3,4,5,6-tetrafluorobenzene (HTM14)



The mixture of **8** (0.82 g, 0.001 mol), bis(4-methoxyphenyl)amine (1.15 g, 0.005 mol), palladium acetate (0.0045 g, 0.00002 mol), tri-tert-butylphosphonium tetrafluoroborate (0.008 g, 0.000027 mol), sodium tert-butoxide (0.48 g, 0.005 mol) in 10 ml of anhydrous toluene was refluxed for 24 hours under argon atmosphere. Afterwards, water was added and the extraction was done with ethyl acetate. The organic layer was dried over anhydrous Na₂SO₄, filtered, and the solvent was evaporated. The crude product was purified by column chromatography using 4:21 v/v acetone/*n*-hexane as an eluent to collect **HTM14** as a yellow solid. The 20% solution of the solid residue in tetrahydrofuran was poured while intensively stirring into a twentyfold excess of methanol. Yield: 0.93 g (66%).

¹H NMR (400 MHz, DMSO, δ, ppm): 7.56 (s, 4H), 7.26-7.15 (m, 4H), 6.97 (d, *J* = 9.1 Hz, 4H), 6.77 (q, *J* = 9.0 Hz, 31H), 5.95 (s, 4H), 3.65 (s, 24H).

¹³C NMR (101 MHz, CDCl₃, δ, ppm): 154.74, 142.39, 137.53, 124.38, 123.52, 115.08, 55.60.

Anal. calcd. for C₃₈H₇₂F₄N₆O₈: C, 74.56; H, 5.12; N, 5.93. Found: C, 74.62; H, 5.09; N, 5.86.

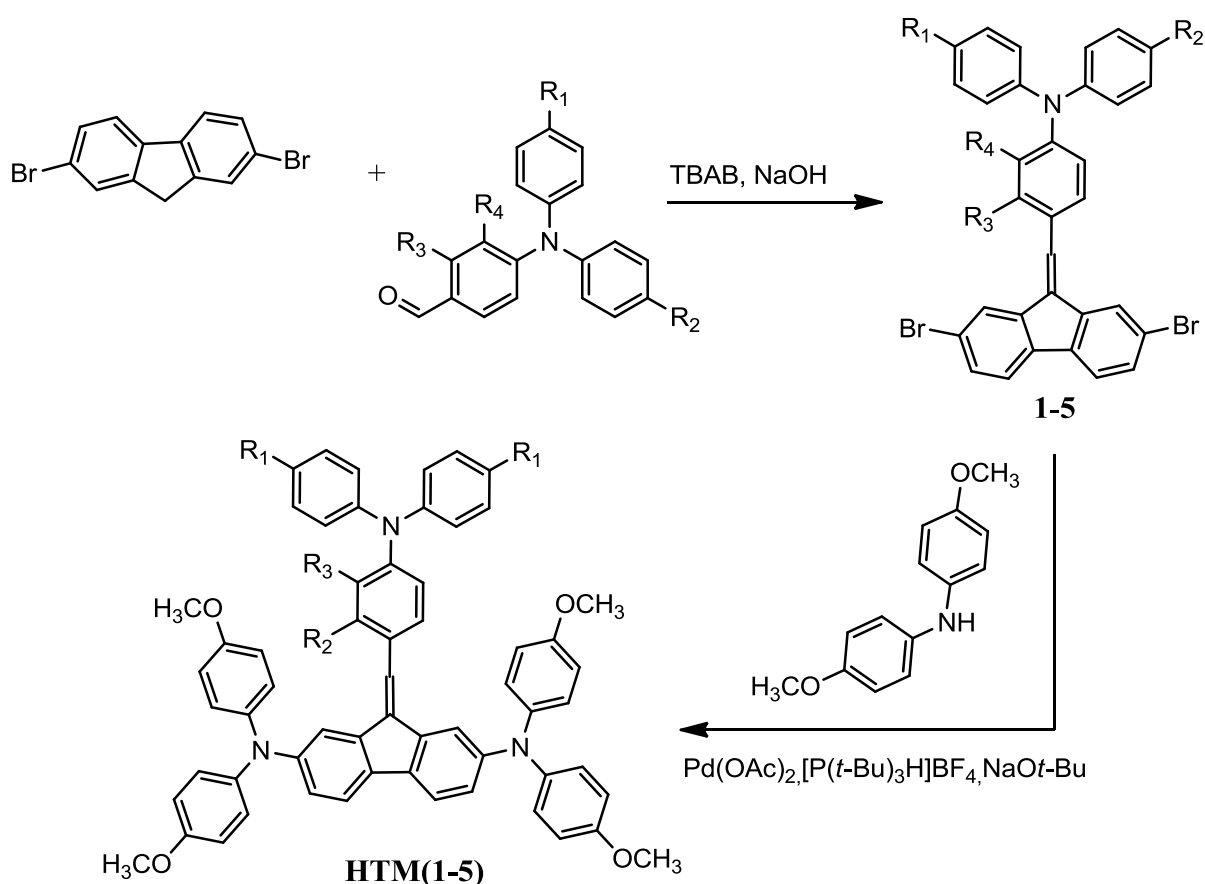
4. RESULTS AND DISCUSSIONS

4.1. HTMs based on fluorene with different aliphatic substitutions

The literature review showed that many new HTMs have been synthesized and investigated, however the industry is still lead by the expensive spiro-OMeTAD [32]. The high cost of this material is determined by factors such as costly reagents, a multistep synthesis and expensive methods used for the purification of the compound [33]. Much work has been put into developing more cost effective HTMs whose performances would rival or exceed those of Spiro-OMeTAD [34-37]. One of the potential paths to simplify the synthesis procedure of hole transporting materials is replacement of the 9,9'-spirobifluorene core with easier alternatives. Compounds containing a fluorene, TPA or carbazole core with methoxydiphenylamine branches have exhibited their efficiency being the most effective HTMs used for PSC construction [38-40]. For this reason, it is fitting to try a combination of two of the three given materials as a new type of HTM to be used in perovskite solar cells. Furthermore, it has been established that the structure of the hole transporting materials has a large impact on charge transport and energy level properties as well as molecular planarity [41]. Therefore, a series of HTMs with different methyl or aliphatic substituents were synthesized in order to study the link between the structure of the hole transporting materials and their photovoltaic efficiency

4.1.1. Synthesis

Synthesis of **HTM1-HTM5** involves two steps the first of which is a simple reaction between 2,7-dibromofluorene with the corresponding formyltriphenylamine [42]. The second reaction is a palladium-catalysed C–N cross coupling reaction between intermediates **1-5** and 4,4'-dimethoxydiphenylamine (**Figure 3**). It was noticed that the substituents did not have a significant effect on the duration of the reaction, however the molecular structure did impact the yield and the purification of the compounds.



- 1, HTM1** $R_1=R_2=R_3=H$;
2, HTM2 $R_1=R_2=H, R_3=CH_3$;
3, HTM3 $R_1=R_3=H, R_2=CH_3$;
4, HTM4 $R_1=CH_3, R_2=R_3=H$;
5, HTM5 $R_1=C_4H_9, R_2=R_3=H$;

Figure 3. Synthesis of **HTM1-HTM5**

A similar hole transporting material was also synthesized by replacing the formyltriphenylamine fragment with a carbazole-based one. The synthesis of the HTM involved the condensation of 2,7-dibromofluorene with 9-ethyl-3-carbazolecarboxyaldehyde. A palladium-catalysed C-N cross coupling reaction between **6** and 4,4'-dimethoxydiphenylamine follows it (**Figure 2**).

It was theorized that an extended π -electron system would improve the properties of an HTM. As a result **HTM1** was used in a simple bromination reaction [43] and the received intermediate compound **7** was used in a Buchwald-Hartwig cross coupling reaction with 4,4'-dimethoxydiphenylamine to synthesize **HTM7** (**Figure 5**).

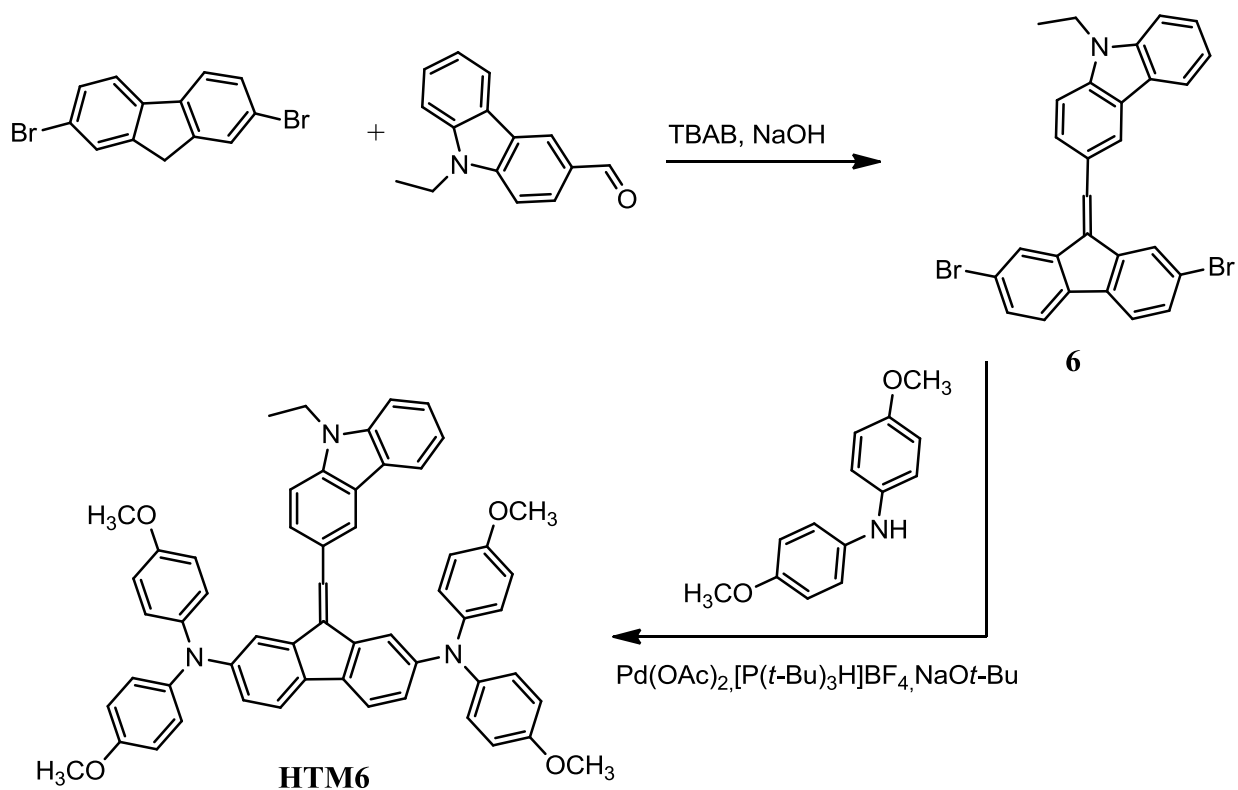


Figure 4. Synthesis of HTM6

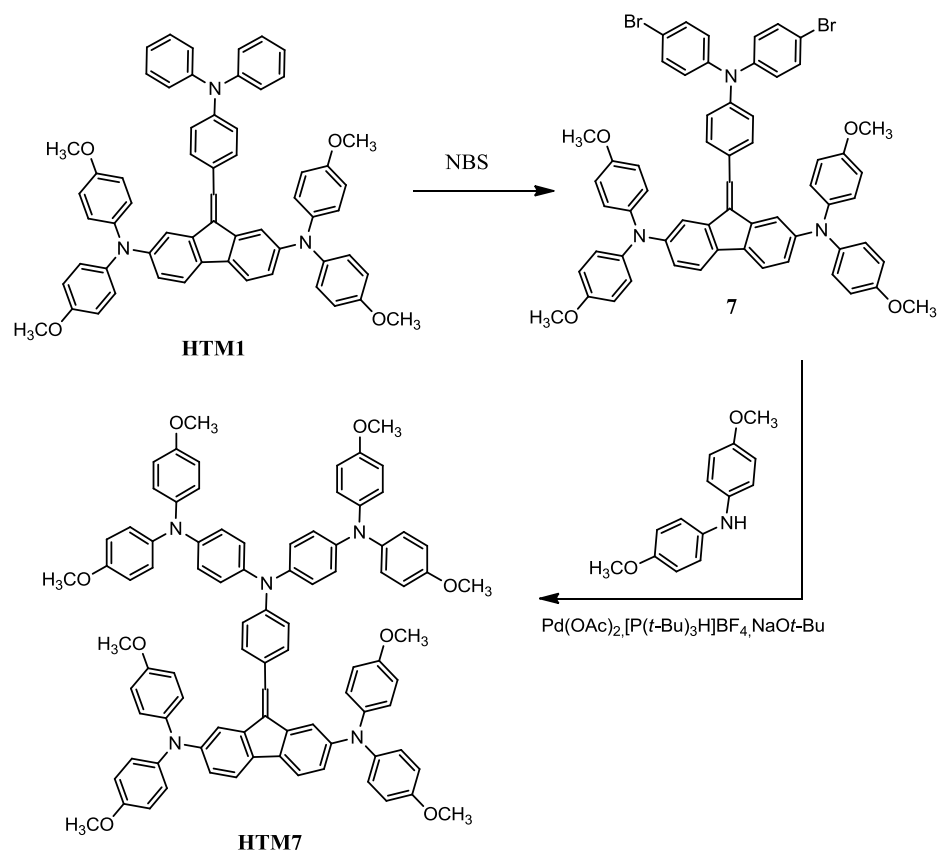


Figure 5. Synthesis of HTM7

4.1.2. Properties

Thermal properties of hole transporting materials **HTM1-HTM7** were determined after performing the differential scanning calorimetry (DSC) and thermogravimetric analysis (TGA). The results are summarized in **Table 1**. The DSC revealed that all the HTMs are molecular glasses as the graph did not exhibit any spikes associated with melting or crystallization. **Figure 6** demonstrates the thermogram of **HTM5**. It can be seen that during both heatings only glass transition temperatures (T_g) are recorded i.e. transformations that are typical for amorphous compounds.

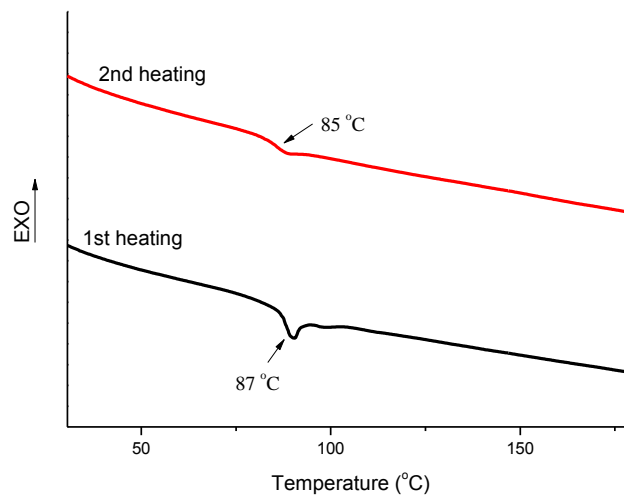


Figure 6. Differential scanning calorimetry first and second heating curves of **HTM5**

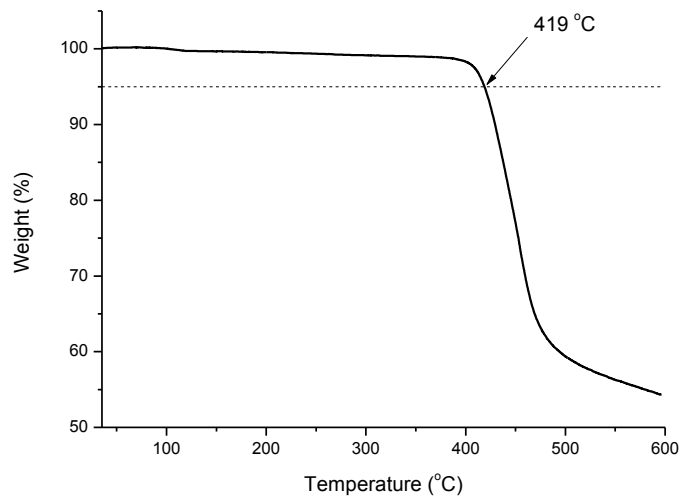
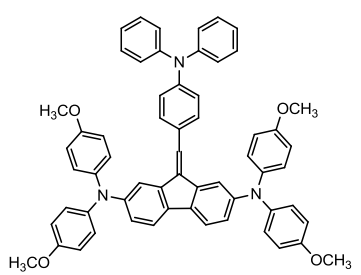
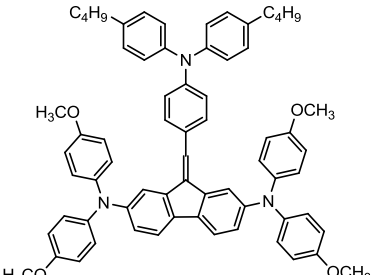
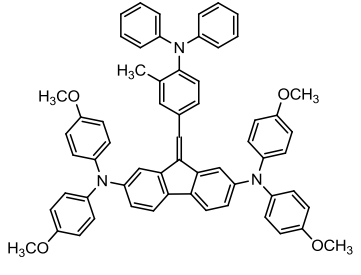
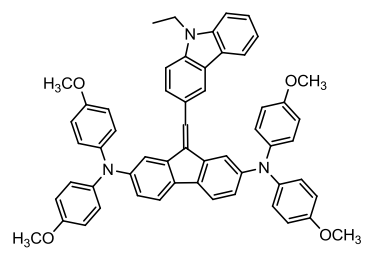
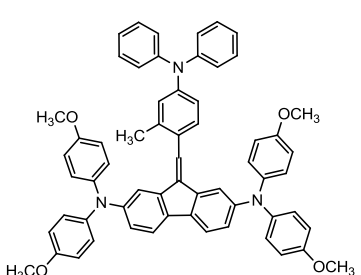
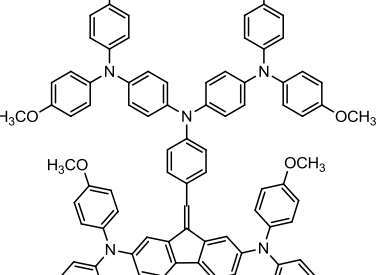
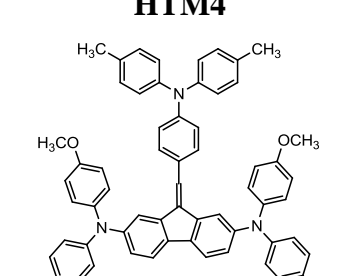


Figure 7. Thermogravimetric heating curve of **HTM2**

Table 1. Thermal properties of the synthesized HTMs. T_g – glass transition temperature, T_{dec} – temperature of 5% thermal decomposition

Material	T_g , °C	T_{dec} , °C	Material	T_g , °C	T_{dec} , °C
<p>HTM1</p> 	108	416	<p>HTM5</p> 	85	413
<p>HTM2</p> 	104	419	<p>HTM6</p> 	127	422
<p>HTM3</p> 	104	418	<p>HTM7</p> 	132	422
<p>HTM4</p> 	89	413			

TGA of the hole transporting materials exhibits excellent thermal stability as all the compounds begin decomposing at temperatures over 410 °C. It is obvious from the data of the DSC analysis that alkyl groups tend to lower the T_g of compounds **HTM2-HTM5**, compared to **HTM1**, most notably in materials **HTM4** and **HTM5**. A symmetrical *p*- substitution in the triphenylamino fragment of the molecule makes the T_g drop by 19 °C and 23 °C in **HTM4** and **HTM5** respectively. This shows that the symmetry of the alkyl substituted molecule has a negative effect on the glass transition temperature. The addition of a single methyl group in the *o*- or *m*- positions of the TPA fragment lowers the glass transition temperature quite insignificantly (**HTM2** and **HTM3**). Compounds **HTM6** and **HTM7** have higher T_g values which can be attributed to a carbazole chromophore **HTM6** and to a larger overall molecule **HTM7**.

All the synthesized materials show two absorption maximums at 293-300 nm and 381-385 nm (**Figure 8**). As expected the largest photon absorption at 300 nm can be seen from **HTM7** as it has the longest conjugated π - π electron system. Materials **HTM1-HTM6** display a relatively large hypochromic effect and slight bathochromic shifts compared to **HTM7**. At around 380 nm the absorption of all compounds seems to be quite similar. The biggest absorption seems to be exhibited by **HTM6** at 381 nm, which may be attributed to the carbazole fragment of the molecule, while other materials show a minor bathochromic shift and slight hypochromic effect. Overall **HTM7** has the highest π electron excitation energy primarily because of the largest conjugated π - π electron system that it possesses.

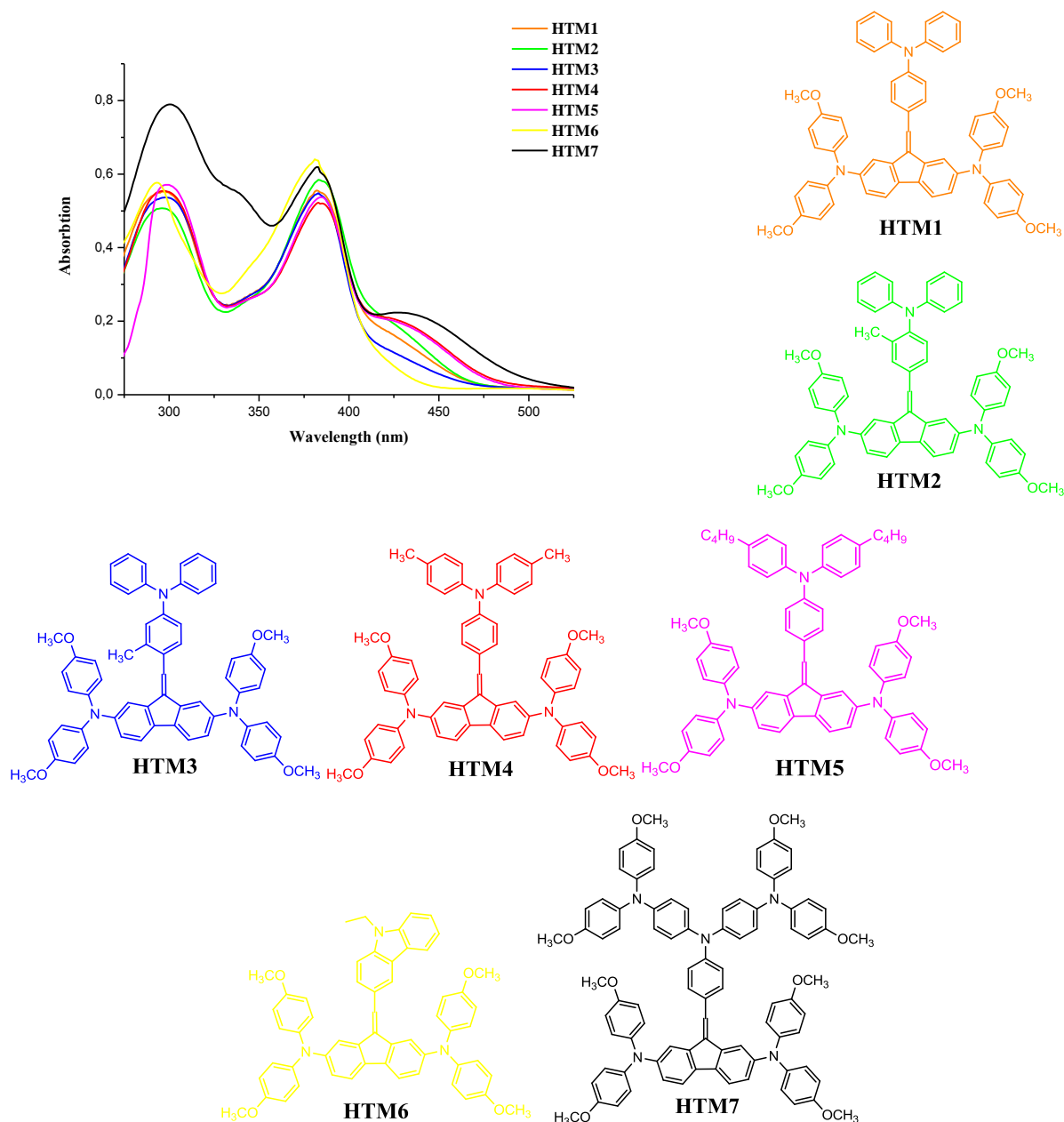


Figure 8. Absorption spectra of **HTM1-HTM7**. Recorded from the 10^{-4} M solution in THF.

Ionization potential (I_p) for materials **HTM1-HTM7** was measured by electron photoemission in air¹ and is presented in **Table 2**. The values vary between 4.92 eV and 5.05 eV. It is evident that the presence of an alkyl group in materials **HTM2-HTM5** lowers the I_p compared to **HTM1**, most notably in **HTM4**. It should be noted that changing the chromophore (**HTM6**) or lengthening the conjugated π - π electron system (**HTM7**) had the same effect on the I_p as did an addition of a single

¹ I_p and μ were measured at the Department of Solid State Electronics, Vilnius University by dr. V. Gaidelis and dr. V. Jankauskas.

methyl group to the molecule (**HTM2**, **HTM3**). The PSC performance depends on whether or not the HTM I_p is lower than the valence band of the perovskite (~ 5.3 eV) [44] thus proving that all of the measured hole transporting materials are suitable for use in perovskite solar cells.

For further investigation of electrical properties of the synthesized materials hole drift mobility was measured by time of flight technique¹ with compounds **HTM1-HTM6**. The results of are presented in **Table 2**. **HTM1** displays the best drift mobility while materials **HTM2** and **HTM4-HTM6** show slightly lower results. The biggest surprise was the inferior mobility of **HTM3**. It might be that the *m*- substitution near the fluorene fragment of the molecule causes a spatial obstruction which leads to molecular packing that is unfavorable for charge transport. The drift mobility values obtained show that compounds **HTM1-HTM2** and **HTM4-HTM6** can be used in solar cells due to the relatively high drift mobility they possess.

Table 2. Ionization potential and drift mobility values of **HTM1-HTM7**. μ - at an electric field of 6.4×10^5 V/cm.

Compound	I_p , eV	μ_0 , (cm ² /V·s)	μ , (cm ² /V·s)
HTM1	5.05	1.4×10^{-5}	6×10^{-4}
HTM2	5.00	1.3×10^{-5}	4×10^{-4}
HTM3	5.00	1.2×10^{-9}	3.5×10^{-7}
HTM4	4.92	2.2×10^{-5}	3.8×10^{-4}
HTM5	5.03	1.1×10^{-5}	3.7×10^{-4}
HTM6	5.00	1×10^{-5}	3.8×10^{-4}
HTM7	5.00	-	-

Compounds **HTM1-HTM5** were used as hole transporting materials in perovskite solar cells². A device using Spiro-OMeTAD was also built as reference. The photovoltaic characteristics of the PSCs are shown in **Table 3**.

Table 3. Short circuit current-density (J_{sc}), open-circuit voltage (V_{oc}), fill factor (FF) and power conversion efficiency (PCE) of materials **HTM1-HTM5** and **spiro-OMeTAD**.

Materials	J_{sc} , mA/cm ²	V_{oc} , mV	FF	PCE, %
HTM1	19.075	1005	75.7	14.52
HTM2	17.526	1146	74.2	15.09
HTM3	13.371	915	70.7	9.15
HTM4	21.269	1052	75.0	16.79
HTM5	21.136	1029	75.7	16.45
Spiro-OMeTAD	21.607	1092	75.3	17.88

The results show that the position of a methyl group in the compound had an evident effect on the performance of the perovskite solar cell. As expected **HTM3** which had the lowest charge mobility exhibited the worst power conversion efficiency. The changing of the positioning of the methyl group from *m*- to *o*- had an obvious effect as the PCE of **HTM2** was 15.09 %. The best results were shown by **HTM4** which reached almost 16.8% in power conversion efficiency, while spiro-OMeTAD displayed 17.88% under the same conditions. This shows that materials such as HTM4 and HTM5 can be used in PSCs as more cost effective alternatives to spiro-OMeTAD.

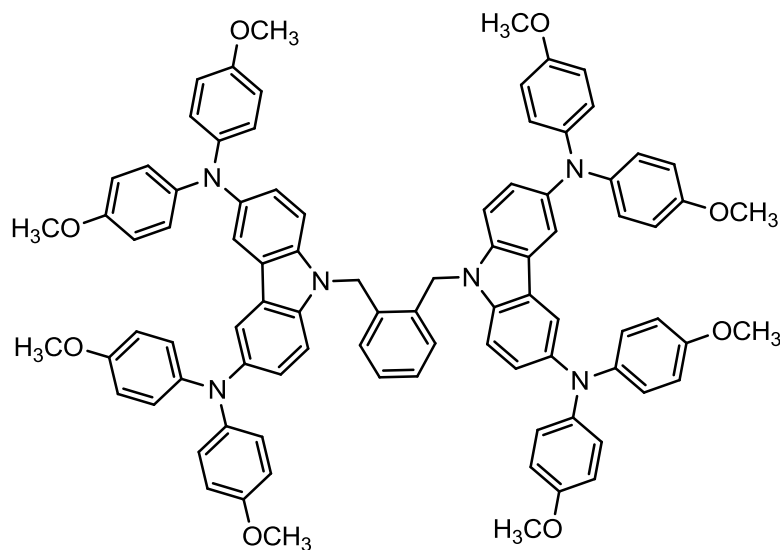
4.1.3. Conclusions

This section displayed easily synthesized fluorene and triphenylamine or carbazole-based HTMs. Optical and thermal properties have been investigated and it was determined that aliphatic substitutions impacted these characteristics. PSCs using materials **HTM1-HTM5** were constructed and it was shown that materials such as **HTM4** and **HTM5** can be used in PSCs and display similar results as well as be more cost effective alternatives to spiro-OMeTAD.

4.2. Fluorinated HTMs

Efficiency has been the main focus in perovskite solar cells while their stability has not been addressed as often. One of the principal problems of PSCs is the hygroscopicity of the the perovskite. When exposed to moisture the perovskite degrades into lead iodide (PbI₂) [45]. In order to address

this problem the knowledge about structure of the PSC was used. Since the HTM layer is on top of the perovskite layer it was theorized that a hydrophobic hole transporting material might increase the stability of the device. Because of the influence of the fluorine atoms to perovskite solar cells mentioned in the literature review it was decided to synthesize a series of molecules based on compounds that show great results in perovskite solar cells: spiro-OMeTAD and V886 [40]. The targeted materials would have several fluorine atoms in their structure hoping that it improves the overall properties compared to the reference compounds.



V886

4.2.1. Synthesis

The synthesis of **HTM8** and **HTM9** involved a simple Buchwald-Hartwig cross coupling reaction between bis(4-(trifluoromethoxy)phenyl)amine and 2,2',7,7'-tetrabromo-9,9'-spirobifluorene or 1,2-Bis(3,6-dibromo-9H-carbazol-9-methyl)benzene respectively (**Figure 9**).

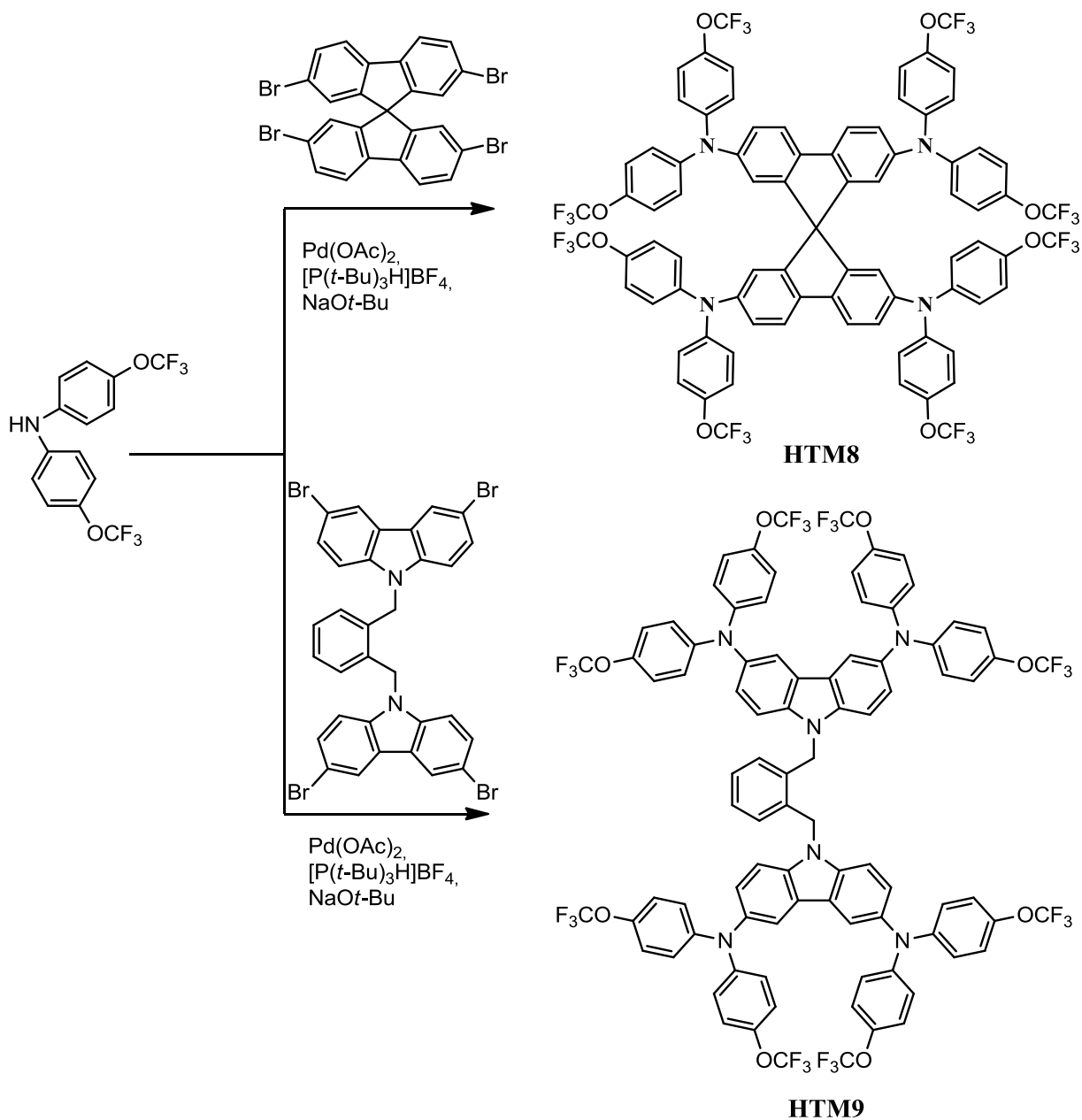


Figure 9. Synthesis of fluorinated compounds **HTM8** and **HTM9**.

Similar compounds to **HTM8** were also synthesized this time replacing hydrogen atoms by fluorine ones in the aromatic fragment of the diphenylamine instead of the methoxy groups. Spiro-OMeTAD-based materials **HTM10-HTM12** were received (**Figure 10**).

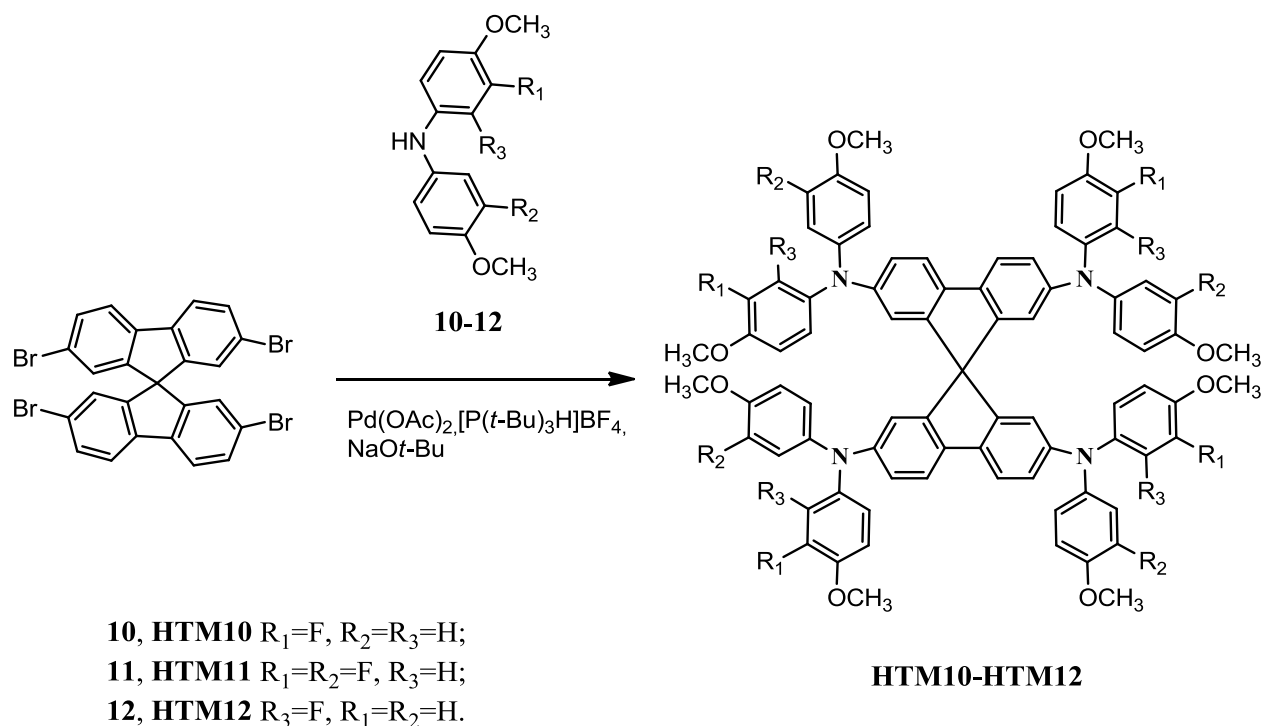


Figure 10. Synthesis of **HTM10-HTM12**.

The purification of compounds **HTM11** and **HTM12** proved to be quite troublesome, for that reason V886 based materials with diphenylamines **11** and **12** were not synthesized. By analogy **HTM13** was also received in a palladium catalyzed C-N cross coupling reaction (**Figure 11**).

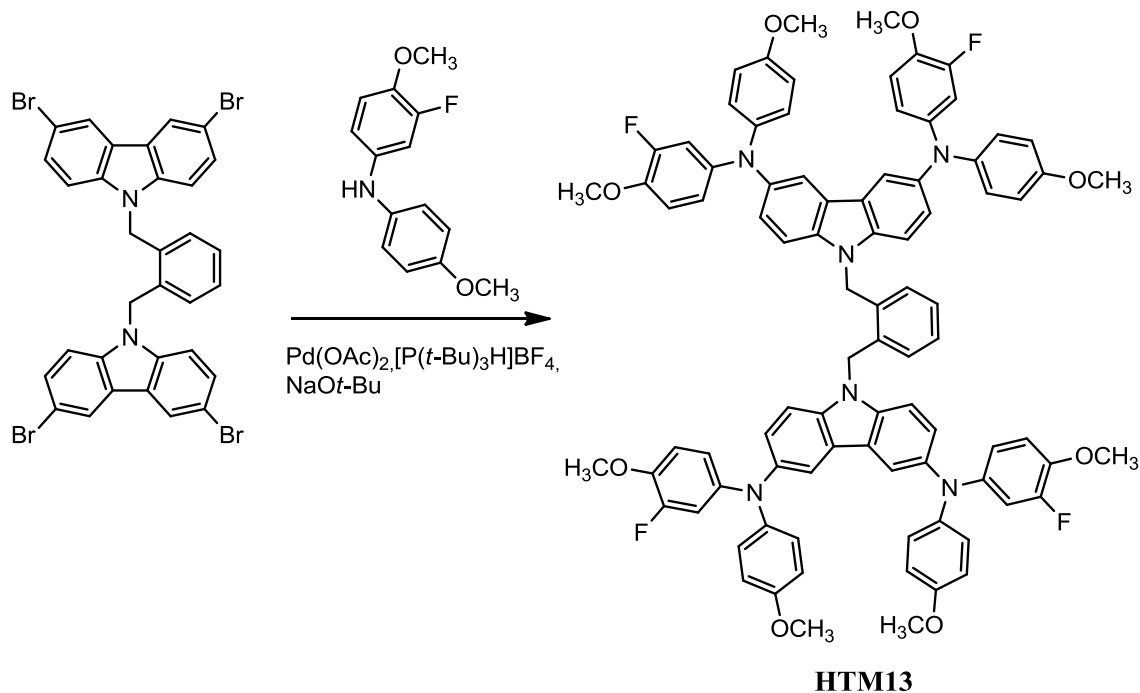


Figure 11. Synthesis of **HTM13**.

As **HTM8-HTM13** all had fluorine atoms in side branches of their respective molecules it was interesting to synthesize a compound with fluorine atoms in the central fragment of the molecule and find out what effect it would have on the properties of the material. The synthesis route involved a known “click” reaction [40] between 3,6-dibromocarbazole and 3,4,5,6-Tetrafluoro-o-xylene dibromide to receive **8** which was later used in the Buchwald-Hartwig cross coupling reaction to get **HTM14**.

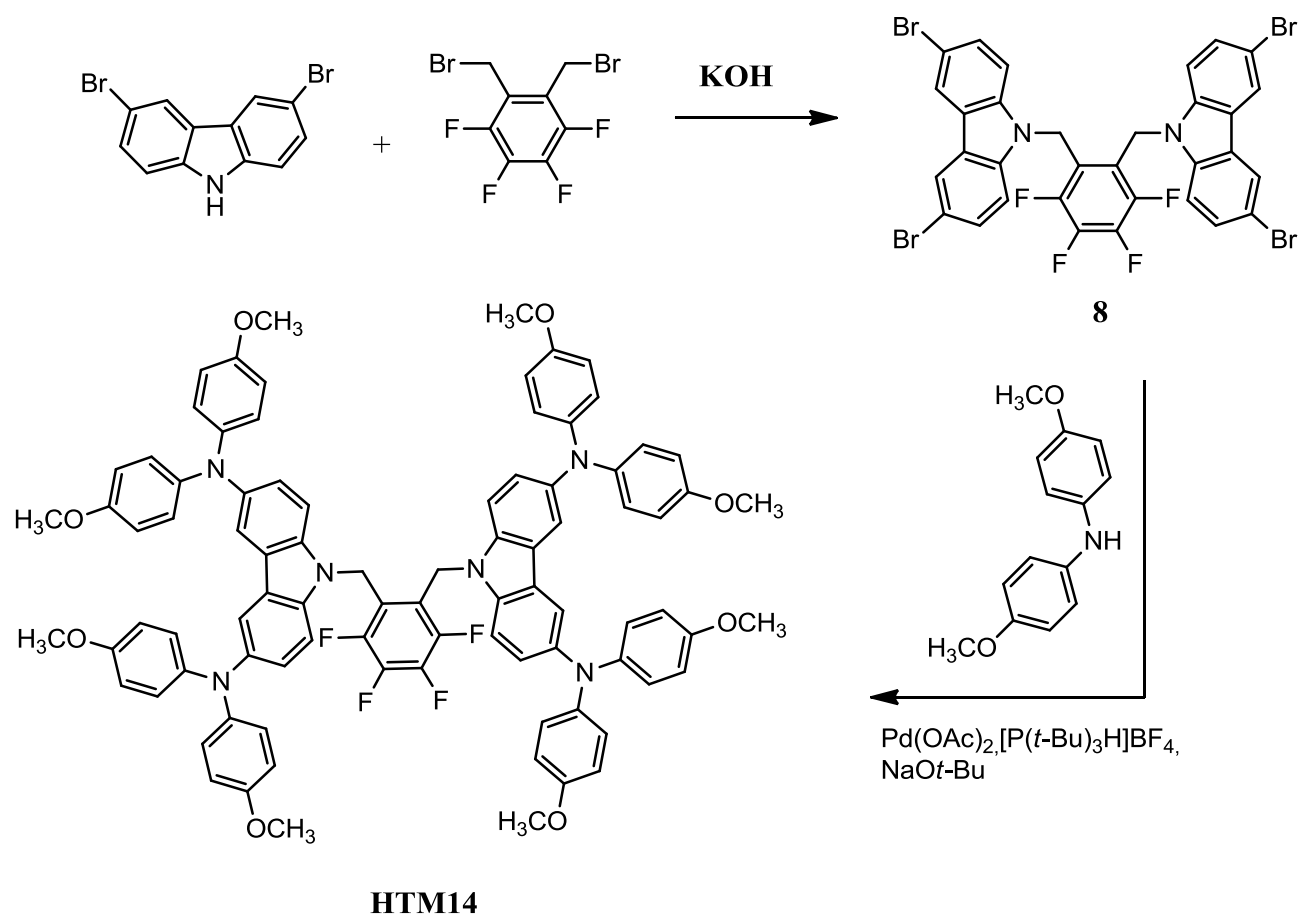


Figure 12. Synthesis of **HTM14**.

4.2.2. Properties

TGA of the spiro-OMeTAD-based materials shows that almost in all instances the addition of fluorine to the molecule lowers the thermal decomposition temperature except for **HTM12**. The decrease of the thermal decomposition temperature in compounds **HTM8**, **HTM10** and **HTM11** directly correlates with the amount of fluorine atoms in the molecule. TGA of the V886-based materials however reveals a different situation. The addition of fluorine atoms to such molecules increases the thermal decomposition temperature in all cases. The DSC analysis of spiro-OMeTAD-

based compounds reveals that substituting hydrogen with fluorine in methoxy groups drastically reduces the glass transition temperature in **HTM8**. Another thing that can be noticed is that **HTM10** has two melting points, after the first one at 227 °C recrystallization happens and it melts again at 265 °C. The DSC analysis of V886-based materials shows that the only notable variation in glass transition temperature is exhibited by **HTM9**.

Table 3. Thermal properties of the fluorinated and reference materials. T_m – melting point temperature.

Compound	T_g , °C	T_m , °C	T_{dec} , °C	Compound	T_g , °C	T_{dec} , °C
HTM8	63	238	380	HTM9	116	400
HTM10	126	227, 265	428	HTM13	138	418
HTM11	186	278	422	HTM14	137	393
HTM12	122	264	446	V886	137	389
Spiro-OMeTAD	105	255	440			

All the spiro-OMeTAD-based compounds show two absorption maximums at 301-307 nm and 370-383 nm (**Figure 13**). As seen from the UV/Vis spectra the addition of fluorine atoms to the molecule brings out varying hypochromic effects and hypsochromic shifts.

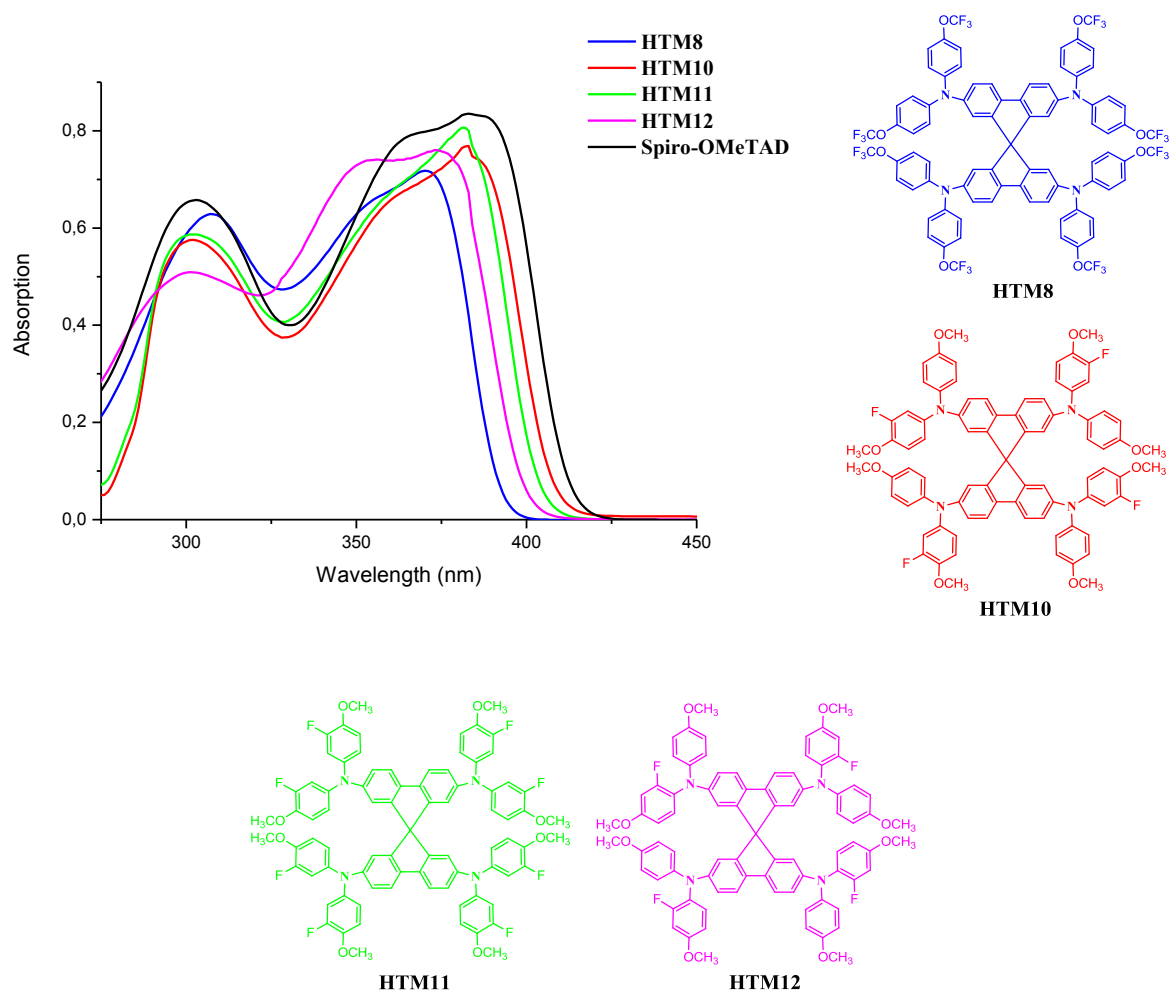


Figure 13. Absorption spectra of Spiro-OMeTAD-based materials. Recorded from the 10^{-4} M solution in THF

The UV/Vis spectra for V886-based compounds shows that all the materials have maximums in the range of 292-303 nm. The most visible hypsochromic shift is exhibited by **HTM13**. Slight hypochromic effects can be seen from fluorinated HTMs compared to V886.

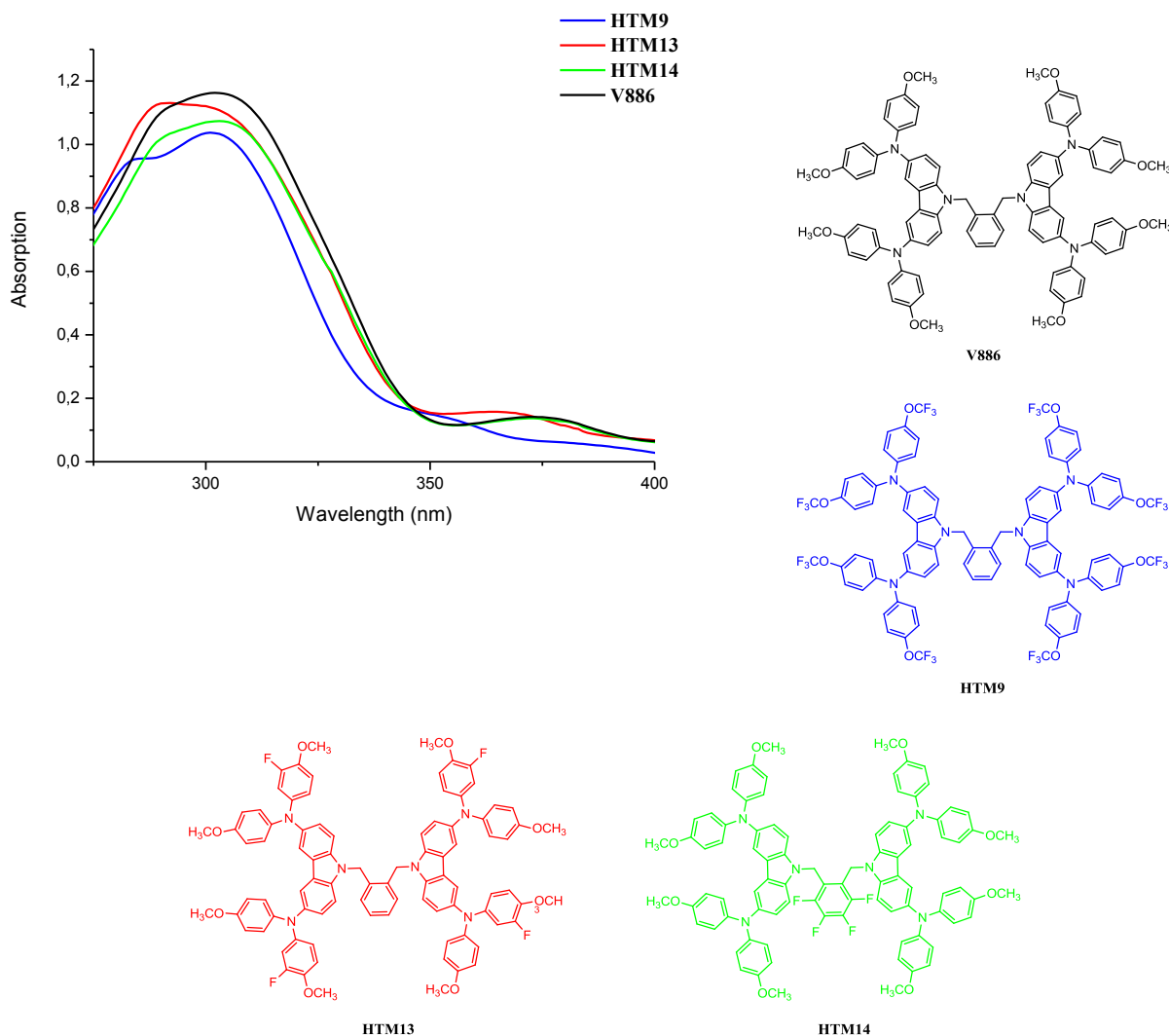


Figure 14. Absorption spectra of V886-based materials. Recorded from the 10^{-4} M solution in THF

I_p for materials **HTM8-HTM14** was measured and their values are presented in **Table 4**. Ionization potentials range from 5.05 eV to 6.20 eV. It is evident that only 4 out of the 7 synthesized materials have suitable I_p values for use in PSCs. The thing that was most unforeseen was the enormous boost to the ionization potential that the trifluoromethoxy groups gave compounds **HTM8** and **HTM9**. In all instances the addition of fluorine atoms to the molecule raised the ionization potential of the material.

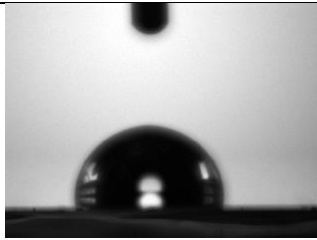
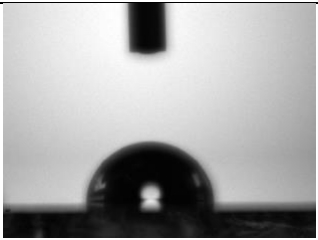
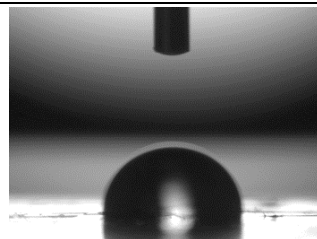
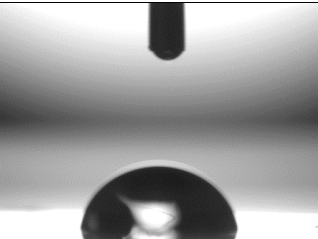
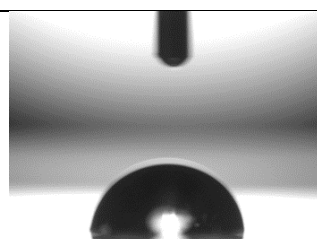
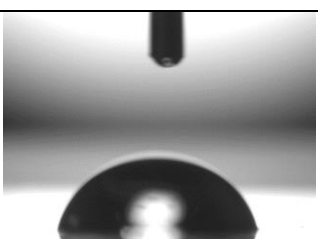
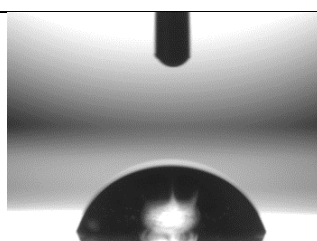
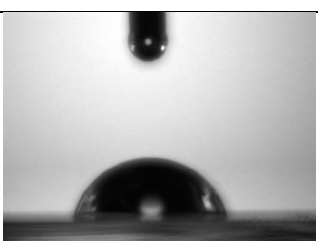
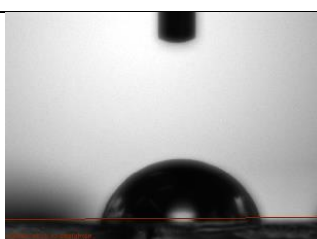
It was attempted to measure hole drift mobility for compounds **HTM8**, **HTM9**, **HTM10** and **HTM13** however only **HTM10** and **HTM13** showed hole mobility. Surprisingly, **HTM8** and **HTM9** both displayed electron mobility, which was unexpected, this demonstrates that a different method should be used to measure the electron mobility for these materials. The results of **HTM10** and **HTM13** revealed that fluorine atoms in these HTMs substantially lowered the hole drift mobility

Table 4 Ionization potential and drift mobility values of fluorinated and reference materials. μ - at an electric field of $6.4 \times 10^5 \text{V/cm}$.

Compound	I_p , eV	μ_0 , ($\text{cm}^2/\text{V}\cdot\text{s}$)	μ , ($\text{cm}^2/\text{V}\cdot\text{s}$)	Compound	I_p , eV	μ_0 , ($\text{cm}^2/\text{V}\cdot\text{s}$)	μ , ($\text{cm}^2/\text{V}\cdot\text{s}$)
HTM8	6.20	-	-	HTM9	6.15	-	-
HTM10	5.26	2.6×10^{-6}	3.6×10^{-4}	HTM13	5.25	3×10^{-7}	9.3×10^{-5}
HTM11	5.41	-	-	HTM14	5.12	-	-
HTM12	5.05	-	-	V886	5.04	2×10^{-5}	6×10^{-4}
Spiro-OMeTAD	5.00	4×10^{-5}	5×10^{-4}				

The wetting angle of compounds **HTM8-HTM14** and reference materials Spiro-OMeTAD and V886 was measured by the sessile drop method and the results are presented in **Table 5**.

Table 5. Wetting angles of the fluorinated and reference materials.

Material	Drop image	Wetting angle, °	Material	Drop image	Wetting angle, °
HTM8		94.2	HTM9		89.8
HTM10		89.1	HTM13		82.3
HTM11		84.8	HTM14		73.1
HTM12		77.3	V886		70.1
Spiro-OMeTAD		82.5			

As evidenced by **Table 5** fluorine atoms in the molecule almost always increase the hydrophobicity of the compound. Out of all the materials only **HTM8** is hydrophobic since only it shows a wetting angle of more than 90° . The biggest surprise was that **HTM12** showed a decreased wetting angle compared to spiro-OMeTAD while containing fluorine atoms in its structure, which may be attributed to such a molecular packaging that decreases the hydrophobicity of the molecule.

4.2.3. Conclusions

This section displayed materials that had several fluorine atoms in their structure. Properties of the synthesized materials were investigated and it was proved that the addition of fluorine groups had both positive and negative effects on the properties of the compounds mostly depending on the quantity of fluorine atoms in the molecule. The addition of a trifluoromethoxy group changed the purpose of the material as those compounds became electron transporting materials instead of hole transporting ones. Overall it was proved that the addition of fluorine atoms worsened the drift mobility of the molecules. The measurement of the wetting angle proved that almost in all instances the fluorine addition increased the hydrophobicity of the materials, **HTM8** even displayed a wetting angle of $>90^\circ$ which shows that it is a hydrophobic compound.

CONCLUSIONS

1. Organic materials containing fluoro and methyl groups were synthesized and their properties were investigated.
2. The results of the research of the materials containing aliphatic substituents showed that:
 - 2.1. All the compounds begin decomposing at temperatures over 410 °C showing excellent thermal stability. Glass transition temperatures vary depending on the substitution, a symmetrical *p*- substitution in the triphenylamino fragment (**HTM4** and **HTM5**) drastically decreases the T_g while an addition of a different chromophore or a larger overall molecule increases the glass transition temperature.
 - 2.2. Compounds **HTM1-HTM7** display similar absorption and ionization potential values, as expected the material with the longest conjugated π - π electron system **HTM7** shows the best absorption. The best hole drift mobility is exhibited by **HTM1** with a value of $6 \times 10^{-4} \text{ cm}^2/\text{V}\cdot\text{s}$ at an electric field of $6.4 \times 10^5 \text{ V/cm}$.
 - 2.3. Perovskite solar cells using materials **HTM1-HTM5** were fabricated and the best result of 16.79% was shown by **HTM4**.
3. The results of the research of the materials containing fluorine atoms showed that:
 - 3.1. The addition of fluorine decreased the absorption of the molecules in all instances.
 - 3.2. Adding fluorine atoms to the molecules more or less increased the ionization potential values of the compounds depending on the location of fluorine atoms in the molecule. A substitution of a methoxy group to a trifluoromethoxy one drastically changed the I_p of the materials, increasing them by more than 1 eV, while also changing the purpose of the compounds **HTM8** and **HTM9** which were electron transporting materials.
 - 3.3. Almost in all cases except in **HTM12** the addition of fluorine proved to be beneficial to the hydrophobicity of the material. Compounds **HTM8** and **HTM9** which had the trifluoromethoxy group showed the best wetting angles of 94.2° and 89.8° respectively.

REFERENCES

1. Grätzel M. Recent Advances in Sensitized Mesoscopic Solar Cells. *Accounts of Chemical Research*. 2009, vol. 42 (11), p. 1788-1798.
2. Kojima A., et al. Organometal Halide Perovskites as Visible-Light Sensitizers for Photovoltaic Cells. *Journal of the American Chemical Society*. 2009, vol. 131 (17), p. 6050–6051.
3. National Center for Photovoltaics. Best Research-Cell Efficiencies. [viewed 2017-05-16]. Available from <http://www.nrel.gov>.
4. Green M. A., Ho-Baillie A. and Snaith H. J. The emergence of perovskite solar cells. *Nature Photonics*. 2014, vol. 8, p. 506-514.
5. Bretschneider S. A., et al. Physical and electrical characteristics of lead halide perovskites for solar cell applications. *APL Materials*. [interactive] 2014, vol. 2, Article no. 040701 [viewed on 2017-05-16]. Available from doi: <http://dx.doi.org/10.1063/1.4871795>.
6. Marinova N., Valero S. and Delgado J. L. Organic and perovskite solar cells: Working principles, materials and interfaces. *Journal of Colloid and Interface Science*. 2017, vol. 488 p. 373-389.
7. Sum T. C. and Mathews N. Advancements in perovskite solar cells: photophysics behind the photovoltaics. *Energy & Environmental Science*. 2014, vol. 7, p. 2518-2534.
8. Correa-Baena J.P., et al. The rapid evolution of highly efficient perovskite solar cells. *Energy & Environmental Science*. 2017, vol. 10, p. 710-727.
9. Yu Z. and Sun L. Recent Progress on Hole-Transporting Materials for Emerging Organometal Halide Perovskite Solar Cells. *Advanced Energy Materials*. [interactive] 2015, vol. 5, Article no. 1500213 [viewed on 2017-05-16]. Available from doi: [10.1002/aenm.201500213](https://doi.org/10.1002/aenm.201500213).
10. Kim H. S. et al. Lead iodide perovskite sensitized all-solid-state submicron thin film mesoscopic solar cell with efficiency exceeding 9%. *Scientific Reports*. 2012 vol. 2, p. 591.
11. Tomkutė-Lukšienė D. Synthesis and properties of hole transporting and light emitting materials possessing diphenylamino and carbazolyl moieties. Doctoral dissertation. KTU, Lithuania, 2014.

12. Malinauskas T. et al. Phenylethenyl-Substituted Triphenylamine: Efficient, Easily Obtainable, and Inexpensive Hole-Transporting Materials. *Chemistry: A European Journal*. 2013, vol. 19, p. 15044-15056.
13. Choi H. et al. Efficient star-shaped hole transporting materials with diphenylethenyl side arms for an efficient perovskite solar cell. *Journal of Materials Chemistry A*. 2014, vol. 2, p. 19136-19140.
14. Choi H. et al. Efficient Perovskite Solar Cells with 13.63 % Efficiency Based on Planar Triphenylamine Hole Conductors. *Chemistry: A European Journal*. Vol. 20 p. 10894-10899.
15. Qin P. et al. Perovskite Solar Cells with 12.8% Efficiency by Using Conjugated Quinolizino Acridine Based Hole Transporting Material. *Journal of the American Chemical Society*. 2014, vol. 136, p. 8516-8519.
16. Cho A. N. Acridine-based novel hole transporting material for high efficiency perovskite solar cells. *Journal of Materials Chemistry A*. 2017, vol. 5, p. 7603-7611.
17. Lv S. et al. Mesoscopic TiO₂/CH₃NH₃PbI₃ perovskite solar cells with new hole-transporting materials containing butadiene derivatives. *Chemical Communications*. 2014, vol. 50, p. 6931-6934.
18. Wang J. et al. Novel hole transporting materials with a linear π -conjugated structure for highly efficient perovskite solar cells. *Chemical Communications*. 2014, vol. 50, p. 5829-5832.
19. Lv S. et al. Simple Triphenylamine-Based Hole-Transporting Materials for Perovskite Solar Cells. *Electrochimica Acta*. 2015, vol. 182, p. 733-741.
20. Kazim S. et al. A dopant free linear acene derivative as a hole transport material for perovskite pigmented solar cells. *Energy & Environmental Science*. 2015, vol. 8, p. 1816-1823.
21. Park S. K. et al. High mobility solution processed 6,13-bis(triisopropyl-silylethynyl) pentacene organic thin film transistors. *Applied Physics Letters*. [interactive] 2007, vol. 91, Article no. 063514 [viewed on 2017-05-16]. Available from doi: <http://dx.doi.org/10.1063/1.2768934>
22. Giri G. et al. Tuning charge transport in solution-sheared organic semiconductors using lattice strain. *Nature*. 2011, vol. 480, p. 504-508.
23. Babudri F. et al. Fluorinated organic materials for electronic and optoelectronic applications: the role of the fluorine atom. *Chemical Communications*. 2007, vol. 10, p. 1003-1022.

24. Liu Y. S. et al. Perovskite Solar Cells Employing Dopant-Free Organic Hole Transport Materials with Tunable Energy Levels. *Advanced Materials*. 2016, vol. 28, p. 440-446.
25. Cho I. et al. Indolo[3,2-b]indole-based crystalline holetransporting material for highly efficient perovskite solar cells. *Chemical Science*. 2017, vol. 8, p. 734-741.
26. Yun J. H. et al. Enhancement of charge transport properties of small molecule semiconductors by controlling fluorine substitution and effects on photovoltaic properties of organic solar cells and perovskite solar cells. *Chemical Science*. 2016, vol. 7, p. 6649-6661.
27. Chen H. et al. One-Step Facile Synthesis of a Simple Hole Transport Material for Efficient Perovskite Solar Cells. *Chemistry of Materials*. 2016, vol. 28, p. 2515-2518.
28. Bi D. et al. Efficient luminescent solar cells based on tailored mixed-cation perovskites. *Science Advances*. [interactive] 2016, vol. 2, Article no. e1501170 [viewed on 2017-05-16]. Available from doi: 10.1126/sciadv.1501170
29. Miyamoto E., Yamaguchi Y. and Yokoyama M. Ionization potential of organic pigment film by atmospheric photoelectron emission analysis. *Electrography*. 1989, vol. 28, p. 364-370.
30. Montrimas E., Gaidelis V. and Pazera A. The discharge kinetics of negatively charged Se electrophotographic layers. *Lithuanian Journal of Physics*. 1966, vol. 6, p. 569-578
31. Tiažkis R. Fluoreno dariniai saulės elementų konstravimui. BSc thesis. KTU, Lithuania, 2015.
32. Yang W. S. et al. High-performance photovoltaic perovskite layers fabricated through intramolecular exchange. *Science*. 2015, vol. 348, p. 1234–1237.
33. Saragi T. P. I. et al. Spiro compounds for organic optoelectronics. *Chemical Reviews*. 2007, vol. 107, p. 1011–1065.
34. Saliba M. et al. A molecularly engineered hole-transporting material for efficient perovskite solar cells. *Nature Energy*. [interactive] 2016, vol. 1, Article no. 15017 [viewed on 2016-05-18]. Available on doi: 10.1038/nenergy.2015.17.
35. Molina-Ontoria A. et al. Benzotrithiophene-Based Hole-Transporting Materials for 18.2% Perovskite Solar Cells. *Angewandte Chemie International Edition*. 2016, vol. 55, p. 6270–6274.

36. Zhang J. et al. Constructive Effects of Alkyl Chains: A Strategy to Design Simple and Non-Spiro Hole Transporting Materials for High-Efficiency Mixed-Ion Perovskite Solar Cells. *Advanced Energy Materials*. 2016, vol. 8, Article no. 1502536.
37. Li H. et al. A simple 3,4-ethylenedioxythiophene based hole-transporting material for perovskite solar cells. *Angewandte Chemie International Edition*. 2014, vol. 53, p. 4085–4088.
38. Saliba M. et al. Incorporation of rubidium cations into perovskite solar cells improves photovoltaic performance. *Science*. 2016, vol. 354, p. 206–209.
39. Bi D. et al. Facile synthesized organic hole transporting material for perovskite solar cell with efficiency of 19.8%. *Nano Energy*. 2016, vol. 23, p. 138–144.
40. Gratia P. et al. A Methoxydiphenylamine-Substituted Carbazole Twin Derivative: An Efficient Hole-Transporting Material for Perovskite Solar Cells. *Angewandte Chemie International Edition*. 2015, vol. 54, p. 11409–11413.
41. Zhang, J. B. et al. Constructive effects of alkyl chains: a strategy to design simple and non-spiro hole transporting materials for high-efficiency mixed-ion perovskite solar cells. *Advanced Energy Materials*. 2016, vol. 6, Article no. 1502536.
42. Petrasinova L. et al. 2-(9H-Fluoren-9ylidenemethyl)thiophene. *Acta Crystallographica*. 2008, vol. E64, p. o274.
43. Wang M. et al. Synthesis and photovoltaic behaviors of benzothiadiazole- and triphenylaminebased alternating copolymers. *Polymer*. 2012, vol. 53, p. 324–332.
44. Abrusci A. et al. High-Performance Perovskite-Polymer Hybrid Solar Cells via Electronic Coupling with Fullerene Monolayers. *Nano Letters*. 2013, vol. 13, p. 3124–3128.
45. Habisreutinger S. N. et al. Carbon Nanotube/Polymer Composites as a Highly Stable Hole Collection Layer in Perovskite Solar Cells. *Nano Letters*. 2014, vol. 14, p. 5561–5568.

LIST OF PUBLICATIONS

1. **Tiazkis R.**, Paek S., Daskeviciene M., Malinauskas T., Saliba M., Nekrasovas J., Jankauskas V., Ahmad S., Getautis V. and Nazeeruddin M. K. Methoxydiphenylamine-substituted fluorene derivatives as hole transporting materials: role of molecular interaction on device photovoltaic performance. *Scientific Reports*. 2017, vol. 7, Article no. 150. Available from: <https://www.nature.com/articles/s41598-017-00271-z>.
2. **Tiažkis R.**, Daškevičienė M. and Getautis V. Fluorinti organiniai puslaidininkiai perovskitiniams saulės. *Chemija ir cheminė technologija : studentų mokslinės konferencijos pranešimų medžiaga*, Kaunas, 2017, ISSN 2538-7332 p. 106-108.
3. **Tiazkis R.**, Daskeviciene M., Malinauskas T., Jankauskas V., Kamarauskas E., Barvainiene B. and Getautis V. Hole transporting materials based on fluorene/triphenylamine moieties. *Program and abstract book of Balticum Organicum Syntheticum 2016*. Riga, 2016, p. 183.
4. **Tiazkis R.**, Daskeviciene M., Malinauskas T., Jankauskas V., Kamarauskas E., Barvainiene B. and Getautis V. Hole transporting molecular glasses containing fluorene/triphenylamine moieties. *Chemistry and chemical technology 2016 book of abstracts*. Vilnius, 2016, p. 189.
5. **Tiazkis R.**, Daskeviciene M., Andriekus T., Malinauskas T., Jankauskas V., Kamarauskas E., Barvainiene B. and Getautis V. Simple hole-transporting materials based on fluorine/triphenylamine moieties. *European conference on molecular electronics 2015 information and conference booklet*. Strasbourg, 2015, P214.
6. **Tiažkis R.**, Daškevičienė M., Andriekus T. and Getautis V. Metilgrupių įtaka fluoreno bei trifenilamino chromoforų turinčių fotolaidžių molekulinų stiklų savybėms. *Chemija ir cheminė technologija : studentų mokslinės konferencijos pranešimų medžiaga*, Kaunas, Technologija, 2014, p. 80-82.
7. **Tiažkis R.**, Daškevičienė M. and Getautis V. Naujo krūvininkus transportuojančio organinio puslaidininkio, skirto kietos būsenos saulės elementams, sintezė. *Studentų mokslinė praktika 2013 konferencijos pranešimų santrauka*. Vilnius, 2013, ISBN 978-9955-613-63, p. 182.
8. **Tiažkis R.**, Daškevičienė M. and Getautis V. Naujo teigiamus krūvininkus transportuojančio molekulinio stiklo iš fluoreno sintezė. *Studentų moksliniai tyrimai 2012/2013 konferencijos pranešimų santrauka II dalis*. Vilnius, 2013, ISBN 978-9955-613-54-1, p. 406-407.